

NACA RM E55K04

UNCLASSIFIED

077

NACA

RESEARCH MEMORANDUM

EFFECT OF DESIGN COMPRESSOR PRESSURE RATIO ON
PERFORMANCE OF HYPOTHETICAL TWO-SPOOL
NUCLEAR-POWERED TURBOJET ENGINES

By James F. Dugan, Jr.

Lewis Flight Propulsion Laboratory
Cleveland, Ohio

CLASSIFICATION CHANGED

~~CONFIDENTIAL~~

CLASSIFICATION CHANGED
UNCLASSIFIED

To

By author *NACA Research* Date *January 27, 1958*
Abstracted in Research Notes 74-27 by *JBC*
Efficiency data - Jan 28, 1958
CLASSIFIED DOCUMENTS
APR 10 1956
t.d. 10, 1957

This material contains information affecting the National Defense of the United States within the meaning of the espionage laws, Title 18, U.S.C., Sections 793 and 794, the transmission or revelation of which in any manner to an unauthorized person is prohibited by law.

NATIONAL ADVISORY COMMITTEE FOR AERONAUTICS

WASHINGTON
April 10, 1956

By authority of TPA # 6-3 Date 12/18/61

UNCLASSIFIED

NACA LIBRARY

LANGLEY AERONAUTICAL LABORATORY
Langley Field, Va.



NATIONAL ADVISORY COMMITTEE FOR AERONAUTICS

~~CONFIDENTIAL~~RESEARCH MEMORANDUMEFFECT OF DESIGN COMPRESSOR PRESSURE RATIO ON PERFORMANCE OF
HYPOTHETICAL TWO-SPOOL NUCLEAR-POWERED TURBOJET ENGINES

By James F. Dugan, Jr.

SUMMARY

Hypothetical two-spool nuclear-powered turbojet engines with sea-level static design compressor total-pressure ratios of 20, 15, and 9 and total-pressure losses between the inner-spool compressor exit and turbine inlet of 10 and 30 percent are considered. Each engine operates with the outer-compressor mechanical speed fixed at its design value and the inner-turbine inlet temperature fixed at its design value of 2160° R. Performance with chemical afterburning at 3500° R and with the afterburner inoperative is calculated for flight Mach numbers of 0 to 0.9 at sea level and 0.9 to 2.32 in the stratosphere.

The following results are for the engines with a constant 10-percent total-pressure loss between the inner-spool compressor and turbine. For operation with the afterburner inoperative, the maximum equivalent net thrust for the 9:1 pressure-ratio engine is about 30 percent greater than that for the 15:1 pressure-ratio engine, and 51 percent greater than that for the 20:1 pressure-ratio engine. At each flight Mach number, however, the higher-pressure-ratio engines have the lower values of specific power (ratio of reactor power to engine net thrust) and require the smaller ducts downstream of the compressor exit.

For operation with afterburning at Mach 2.32, thrust for the 9:1 pressure-ratio engine is about 8 and 18 percent greater than the thrust for the 15:1 and 20:1 pressure-ratio engines, respectively; whereas the specific fuel consumption advantage of the 9:1 engine is about 8 and 16 percent, respectively. Specific power, however, for the 20:1 pressure-ratio engine is about 25 and 41 percent less than the specific power for the 15:1 and 9:1 pressure-ratio engines, respectively.

UNCLASSIFIED

~~CONFIDENTIAL~~ AL

~~CONFIDENTIAL~~

INTRODUCTION

The selection of the design compressor total-pressure ratio for a turbojet engine depends on many factors - such as, the allowable turbine inlet temperature, the attainable performance of the turbojet components, the assigned mode of engine operation, the anticipated range of flight conditions, the size and weight of the engine components, and the equilibrium and transient performance of the engine over the full range of operation. The purpose of this report is to estimate the effect of design compressor total-pressure ratio on the equilibrium performance of hypothetical two-spool turbojet engines.

Two series of two-spool engines are considered: The first series is characterized by a 30-percent total-pressure loss between the inner-spool compressor and turbine; the second series, by a 10-percent total-pressure loss. For each series, the sea-level static design over-all compressor total-pressure ratios are 20, 15, and 9, and the design value of the inner-turbine inlet temperature is 2160° R. These values of pressure loss, compressor pressure ratio, and turbine inlet temperature are realistic for a direct-air-cycle type of nuclear-power aircraft engine.

The compressor performance maps of each engine are obtained analytically by the procedures discussed in reference 1. Each of the turbines is characterized by constant inlet equivalent weight flow and constant efficiency for all engine operation. The pumping characteristics of each engine are obtained by matching the compressor and turbine components for a specific mode of operation in which inner-turbine inlet temperature and outer-compressor mechanical speed are held constant at their design values for all flight conditions. The advantages of this mode of operation are discussed in reference 2. The performance of each engine with chemical afterburning at 3500° R and with the afterburner inoperative is calculated for flight Mach numbers of 0 to 0.9 at sea level and 0.9 to 2.32 in the stratosphere.

The equilibrium operating lines corresponding to the assigned mode of operation and range of flight conditions are plotted on the component compressor maps to indicate the variations in compressor efficiency and the margins between the operating lines and the stall-limit lines. The performance of the gas generators (that part of the engine from the outer-compressor inlet to the outer-turbine exit) is presented in order that performance may be calculated for engines having inlet and exhaust-nozzle characteristics different from those of this report. The performances of three engines, each with a design compressor total-pressure

~~CONFIDENTIAL~~

3909

ratio of 20, are compared to indicate the effects of varying the design-pressure-ratio split and of assigning the engine design point on the outer-compressor performance map away from the outer-compressor peak polytropic efficiency point.

The performances of engines with the same percentage total-pressure loss between the inner-spool compressor and turbine but different values of design compressor total-pressure ratio are compared to indicate the effect of design compressor total-pressure ratio on the variations of engine net thrust, specific power, and specific fuel consumption with flight condition. The effect of percentage total-pressure loss between the inner-spool compressor and turbine on engine performance is found by comparing the performances of engines having the same value of design compressor total-pressure ratio but different values of percentage total-pressure loss.

METHOD OF ANALYSIS

Engine Design Conditions

The two-spool turbojet engines considered herein are characterized by the following sea-level static design values:

- Over-all compressor total-pressure ratio 9, 15, or 20
- Outer-compressor equivalent weight flow, lb/sec 100
- Ratio of inner-turbine inlet total-pressure to inner-compressor outlet total pressure 0.7 or 0.9
- Inner-turbine inlet total temperature, R 2160

Eight two-spool engines are discussed in this report. The engine designations and the design values of outer-compressor and inner-compressor total-pressure ratio are listed in the following table:

Engine designation	Outer-compressor pressure ratio at engine design point	Inner-compressor pressure ratio at engine design point
<u>20.7a</u>	4	5
<u>20.7b</u>	5	4
<u>20.7c</u>	4.185	4.779
<u>15.7</u>	2.857	5.250
<u>9.7</u>	2.857	3.150
<u>20.9</u>	4.185	4.779
<u>15.9</u>	2.857	5.250
<u>9.9</u>	2.857	3.150

3909

CF-1 BACK

The engine designation indicates the design compressor total-pressure ratio and the total-pressure ratio between the inner-compressor exit and the inner-turbine inlet. For example, the engine designation 20.7 means the design compressor total-pressure ratio is 20, and the total-pressure ratio P_4/P_3 is 0.7. (The symbols used in this report are defined in the appendix.) The letters a, b, and c which follow 20.7 are used to distinguish three different pressure-ratio divisions between the outer and the inner compressors.

For both engines 20.7a and 20.7b, the engine design values of outer-compressor and inner-compressor pressure ratio were assigned to coincide with the outer- and inner-compressor reference points. As used in this report, the compressor reference point of a compressor map is defined as that point at which maximum polytropic efficiency is achieved. For both engines 20.7a and 20.7b, outer-compressor surge was encountered before the full range of operation was covered.

In order to permit operation over the full range of flight conditions, a third engine with a design compressor total-pressure ratio of 20 was considered in which the outer-compressor engine design point differs from the compressor reference point. In engine 20.7c, the outer-compressor engine design point is at a pressure ratio of 4.185 and an equivalent weight flow of 100 pounds per second; while the compressor reference point (maximum polytropic efficiency point) is at a pressure ratio of 4.472 and an equivalent weight flow of 97 pounds per second. By shifting the outer-compressor engine design point to a higher weight flow than that for the compressor reference point, the outer compressor operates in a stable portion of its performance map over the full range of flight conditions. This is done for each of the remaining five two-spool engines; that is, the engine design equivalent weight flow is 100 pounds per second, while the outer-compressor reference-point equivalent weight flow is 97 pounds per second.

Mode of Operation and Range of Flight Conditions

For a particular flight condition, the operation of a two-spool turbojet engine is fixed by assigning two quantities, such as outer-compressor mechanical speed and inner-turbine inlet temperature. In this report, outer-compressor mechanical speed and inner-turbine inlet temperature are assigned to be constant at their design values for the full range of flight conditions. Flight Mach number is varied from 0 to 0.9 at sea level, and from 0.9 to 2.32 in the stratosphere.

Compressor and Turbine Performance

Each compressor map was obtained in three steps: (1) The backbone or line of maximum efficiency was found. (2) The stall-limit line was found. (3) The lines of constant equivalent speed were found.

To carry out step (1), the backbone characteristic curves of reference 1 were employed. In reference 1, relative backbone values of equivalent weight flow, total-pressure ratio, and efficiency are plotted against reference-point pressure ratio with equivalent speed as a parameter. To calculate the backbone values for a particular compressor, the values read from the curves for the reference-point pressure ratio are multiplied by the compressor reference-point values of equivalent weight flow, total-pressure ratio, and efficiency. The compressor reference-point polytropic efficiency is assigned to be 0.90 for each compressor map.

To carry out step (2), the stall-limit-line characteristic curves of reference 1 were employed. In these curves, the ratio of stall-limit pressure ratio to reference-point pressure ratio is plotted against reference-point pressure ratio for constant values of the ratio of stall-limit equivalent weight flow to reference-point equivalent weight flow. The stall-limit line of a particular compressor is calculated by multiplying the values read from the curve for the reference-point pressure ratio by the reference-point values of pressure ratio and equivalent weight flow.

To carry out step (3), the constant-speed characteristic curves of reference 1 were employed. In these curves, relative efficiency and relative temperature rise are plotted against a relative flow parameter. The lines of constant speed for a particular compressor performance map are calculated as follows: For each speed, relative values of flow parameter are assigned and relative values of temperature rise and efficiency are read from the constant-speed curves. Absolute values are calculated from these relative values and the appropriate backbone values. Compressor pressure ratio is calculated from the values of temperature rise and efficiency, and compressor weight flow is calculated from values of temperature ratio, pressure ratio, and flow parameter. Each compressor map is assumed to be valid for all flight conditions; therefore, any effects of flow distortion or low Reynolds number are neglected.

Each of the turbines is characterized by constant inlet equivalent weight flow and a constant polytropic efficiency of 0.90 for all operation. The results of reference 2 show that, for an operating mode characterized by constant values of outer-compressor mechanical speed and inner-turbine inlet temperature, the inner turbine operates very close to its design point for the full range of flight conditions; that is, inner-turbine inlet equivalent weight flow remains constant at its design value and inner-turbine efficiency varies less than 1 percent. The outer turbine of the two-spool engine of reference 2 operates at its design value of inlet equivalent weight flow and near its design value of efficiency for all flight conditions considered. On the basis of these results, the turbine assumptions of this report are believed to be good.

Gas-Generator Performance

The variations of compressor inlet equivalent weight flow $w_1 \sqrt{\theta_1}/\delta_1$, compressor exit equivalent weight flow $w_3 \sqrt{\theta_3}/\delta_3$, compressor temperature ratio T_3/T_1 , engine temperature ratio T_6/T_1 , and engine pressure ratio P_6/P_1 with outer-compressor equivalent speed $N_o/\sqrt{\theta_1}$ are obtained for the specified mode of operation in which the inner-turbine inlet temperature and the outer-compressor mechanical speed are held constant at their design values for all flight conditions. This mode of operation results in a unique relation between T_4/T_1 and $N_o/\sqrt{\theta_1}$. For each speed $N_o/\sqrt{\theta_1}$, the inner-turbine inlet to outer-compressor inlet temperature ratio T_4/T_1 is calculated from

$$\frac{T_4}{T_1} = \frac{\left(\frac{N_o}{\sqrt{\theta_1}}\right)^2 \left(\frac{T_4}{T_1}\right)_d}{\left(\frac{N_o}{\sqrt{\theta_1}}\right)_d^2} \quad (1)$$

The variations of $w_1 \sqrt{\theta_1}/\delta_1$, $w_3 \sqrt{\theta_3}/\delta_3$, T_3/T_1 , P_6/P_1 , and T_6/T_1 with $N_o/\sqrt{\theta_1}$ are found by first matching the inner compressor and inner turbine, and then matching the inner spool with the outer compressor and outer turbine.

Inner-spool matching. - The performance of the inner spool is found as follows:

(1) A value of $w_2 \sqrt{\theta_2}/\delta_2$ is assigned at a particular speed $N_i/\sqrt{\theta_2}$.

(2) The values of P_3/P_2 and T_3/T_2 are read from plots of these variables against $w_2 \sqrt{\theta_2}/\delta_2$, with $N_i/\sqrt{\theta_2}$ as parameter.

(3) The value of T_4/T_2 is calculated from

$$\frac{T_4}{T_2} = \left[\frac{\left(\frac{w_4 \sqrt{\theta_4}}{\delta_4}\right)_d \left(\frac{P_4}{P_3}\right)_d \frac{P_3}{P_2}}{w_2 \sqrt{\theta_2}/\delta_2} \right]^2 \quad (2)$$

(4) The value of T_5/T_4 is calculated from

$$\frac{T_5}{T_4} = 1 - \frac{c_{p,2} \left(\frac{T_3}{T_2} - 1 \right)}{c_{p,4} \frac{T_4}{T_2}} \quad (3)$$

If the value of T_5/T_4 from step (4) does not equal the design value, steps (1) to (4) are repeated. The value of T_5/T_4 for all operating conditions must be a constant equal to the design value because the values of $w_4 \sqrt{\theta_4}/\delta_4$, $w_5 \sqrt{\theta_5}/\delta_5$, and η_{4-5} are assigned to be constant for all operating conditions. When T_5/T_4 from step (4) equals the design value, the inner-compressor operating point is compatible with the specified turbine assumptions.

Inner-spool performance is presented as plots of $w_2 \sqrt{\theta_2}/\delta_2$, T_3/T_2 , P_3/P_2 , P_5/P_2 , T_5/T_2 , and T_4/T_2 against $N_1/\sqrt{\theta_2}$.

Inner-spool matching with outer-spool components. - The inner-spool is matched with the outer-spool components as follows:

(1) A value of $w_2 \sqrt{\theta_2}/\delta_2$ is assigned at a particular speed $N_0/\sqrt{\theta_1}$.

(2) At this value of $w_2 \sqrt{\theta_2}/\delta_2$, values of $N_1/\sqrt{\theta_2}$, T_3/T_2 , P_3/P_2 , P_5/P_2 , T_5/T_2 , and T_4/T_2 are read from the inner-spool performance curves.

(3) A value of T_2/T_1 is read from the plot of T_2/T_1 against $w_2 \sqrt{\theta_2}/\delta_2$, with $N_0/\sqrt{\theta_1}$ as parameter.

(4) A value of T_4/T_1 is calculated from the values of T_4/T_2 and T_2/T_1 . If this value does not equal that calculated from equation (1), steps (1) to (4) are repeated. When the values of T_4/T_1 agree, the outer-compressor and inner-compressor operating points are compatible with the assigned mode of operation.

At each speed $N_0/\sqrt{\theta_1}$, the value of $w_1 \sqrt{\theta_1}/\delta_1$ is read from a plot of $w_1 \sqrt{\theta_1}/\delta_1$ against $w_2 \sqrt{\theta_2}/\delta_2$ for constant values of $N_0/\sqrt{\theta_1}$. The value of $w_3 \sqrt{\theta_3}/\delta_3$ is calculated from the values of $w_2 \sqrt{\theta_2}/\delta_2$, T_3/T_2 , and P_3/P_2 . The value of T_3/T_1 is calculated from the values

of T_2/T_1 and T_3/T_2 . The value of P_6/P_1 is calculated from the values of P_2/P_1 , P_5/P_2 , and P_6/P_5 , where the value of P_6/P_5 is calculated from

$$\frac{P_6}{P_5} = \left[1 - \frac{c_{p,1} \left(\frac{T_2}{T_1} - 1 \right)}{c_{p,5} \frac{T_5}{T_1} \eta_{5-6}} \right] \gamma_5^{-1} \quad (4)$$

The value of T_6/T_1 is calculated from the values of T_2/T_1 , T_5/T_2 , and T_6/T_5 , where T_6/T_5 is calculated from

$$\frac{T_6}{T_5} = 1 - \frac{c_{p,1} \left(\frac{T_2}{T_1} - 1 \right)}{c_{p,5} \frac{T_5}{T_1}} \quad (5)$$

Compressor Operating Lines

Equilibrium operating lines are located on the outer- and inner-compressor maps from gas-generator plots of P_2/P_1 , $w_1 \sqrt{\theta_1}/\delta_1$, P_3/P_2 , and $w_2 \sqrt{\theta_2}/\delta_2$ against $N_o/\sqrt{\theta_1}$. The relation between outer-compressor equivalent speed and flight condition for the assigned mode of operation is found as follows: Engine inlet temperature is calculated from

$$T_1 = t_0 \left(1 + \frac{\gamma - 1}{2} M_0^2 \right) \quad (6)$$

where t_0 is the ambient temperature at the specified altitude and M_0 is the specified flight Mach number. (At sea level, t_0 is 518.7° R; in the stratosphere, 390.0° R.) The outer-compressor equivalent speed corresponding to the assigned flight condition is calculated from

$$\frac{\frac{N_o}{\sqrt{\theta_1}}}{\left(\frac{N_o}{\sqrt{\theta_1}} \right)_d} = \sqrt{\frac{518.7}{T_1}} \quad (7)$$

Engine Performance

Thrust, specific power, and specific fuel consumption (for chemical afterburning at 3500° R) are calculated for each engine over the range of flight conditions by the following procedure:

(1) For an assigned flight condition, the values of $N_o/\sqrt{\theta_1}$ is calculated from equation (7), and the value of T_4/T_1 is calculated from equation (1).

(2) Values of $w_1\sqrt{\theta_1}/\delta_1$, P_6/P_1 , and T_6/T_1 are read from the gas-generator performance curves for the known value of $N_o/\sqrt{\theta_1}$.

(3) Inlet total-pressure ratio P_1/P_0 is read from figure 1, which is a calculated plot of P_1/P_0 against M_0 for a variable-geometry inlet having two adjustable wedges and a by-pass duct.

(4) The value of P_0/P_0 is calculated from

$$\frac{P_0}{P_0} = \left(1 + \frac{\gamma - 1}{2} M_0^2\right)^{\frac{\gamma}{\gamma - 1}} \quad (8)$$

(5) Exhaust-nozzle pressure ratio is calculated from

$$\frac{P_7}{P_0} = \frac{P_0}{P_0} \frac{P_1}{P_0} \frac{P_6}{P_1} \frac{P_7}{P_6}$$

where P_7/P_6 is assumed equal to 0.96 with the afterburner inoperative, and 0.94 with afterburning.

(6) Jet velocity is calculated from

$$V_j = C_V \sqrt{\frac{2gR\gamma_7}{\gamma_7 - 1} T_7 \left[1 - \left(\frac{P_0}{P_7}\right)^{\frac{\gamma_7 - 1}{\gamma_7}}\right]} \quad (9)$$

where $T_7 = T_6$ for nonafterburning operation, $T_7 = 3500^\circ$ R for afterburning operation, and $C_V = 0.96$ for both cases.

(7) Net thrust is calculated from

$$F_n = \frac{w_1}{g} [(1 + f)V_j - V_0] \quad (10)$$

where w_1 is calculated from values of $w_1 \sqrt{\theta_1/\delta_1}$, T_1 , and P_1 , and the flight velocity is calculated from

$$V_0 = M_0 \sqrt{\gamma g R t_0} \quad (11)$$

The fuel-air ratio is zero when the afterburner is inoperative. For afterburning operation, the value of fuel-air ratio for the afterburner is found by using figure 2 of reference 3. Afterburner efficiency is taken as 0.90, and the fuel is assumed to have a lower heating value of 18,700 Btu per pound and a hydrogen-carbon ratio of 0.175.

(8) Values of specific power (which is the ratio of the power added to the airstream between the inner-compressor exit and the inner-turbine inlet to the engine net thrust) in kilowatts per pound thrust are calculated from

$$sp = \frac{1.055 w_1 (H_4 - H_3)}{F_n} \quad (12)$$

where the values of H_3 and H_4 are found from the values of T_3 and T_4 and the tables of reference 4.

(9) For afterburning operation, specific fuel consumption is calculated from

$$sfc = \frac{3600 f}{F_n/w_1} \quad (13)$$

RESULTS AND DISCUSSION

Compressor Operating Lines

The variation of outer-compressor equivalent speed with flight condition for operation at constant outer-compressor mechanical speed is shown in figure 2. At sea level, as flight Mach number increases from 0 to 0.9, outer-compressor equivalent speed decreases from 100 to 92.8 percent design. In the stratosphere, as flight Mach number increases from 0.9 to 2.32, outer-compressor equivalent speed decreases from 107 to 80 percent design.

Component compressor maps of the eight two-spool engines are shown in figures 3 to 5, where total-pressure ratio is plotted against inlet equivalent weight flow with equivalent speed and adiabatic efficiency as parameters. On each map is plotted the equilibrium operating line corresponding to the assigned mode of engine operation. Four points are noted on each operating line: Point A (the sea-level static design point) is for Mach 0 at sea level or Mach 1,284 in the stratosphere. Point B is for Mach 0.9 at sea level. Point C is for Mach 0.9 in the stratosphere. Point D is for Mach 2.32 in the stratosphere. If Mach 2.32 is unattainable in a particular engine because of complete compressor stall, point D' is used to note the intersection of the operating line with the compressor stall-limit line.

Engines 20.7a, 20.7b, 20.7c, and 20.9. - Compressor maps of the engines with a design compressor total-pressure ratio of 20 are shown in figure 3. The outer-compressor performance maps of engines 20.7a and 20.7b are shown in figures 3(a) and (b), respectively. For both engines, the engine design point A coincides with the compressor reference point (peak polytropic efficiency point). The variation of outer-compressor efficiency and the location of the operating line with respect to the stall-limit line are similar for the two engines. For the particular compressor maps used, the equilibrium operating line intersects the outer-compressor stall-limit line at an equivalent speed $N_o/\sqrt{\theta_1}$ between 80 and 90 percent design. The intersection corresponds to a flight Mach number of 1.925 for engine 20.7a, and 1.972 for engine 20.7b.

The outer-compressor map of engines 20.7c and 20.9 is shown in figure 3(c). The compressor maps and operating lines for the engines with 10-percent total-pressure loss between the inner-spool compressor and turbine are the same as those for the corresponding engines with 30-percent total-pressure loss. For engines 20.7c and 20.9, the engine design point A was assigned at a higher equivalent weight flow than the peak polytropic efficiency point (compressor reference point) so as to permit stable operation over the full range of flight conditions. The degree to which this compromise should be made will depend on the particular engine being considered. For engines 20.7c and 20.9, the engine design weight flow was assigned to be 100 pounds per second, while the compressor reference weight flow was assigned to be 97 pounds per second. For the particular compressor maps used, this resulted in an equilibrium operating line that intersects the stall-limit line at an outer-compressor equivalent speed of 80 percent design (point D in fig. 3(c)). If a greater margin between engine design weight flow and compressor reference weight flow were assigned, (1) the margin between the operating line and the stall-limit line would increase at all equivalent speeds, (2) the equivalent weight flow at equivalent speeds $N_o/\sqrt{\theta_1}$ below design would increase, and (3) the compressor efficiency at the lower equivalent speeds $N_o/\sqrt{\theta_1}$ would increase and that at the higher equivalent speeds would decrease. The outer-compressor efficiency of engines

20.7c and 20.9 is practically constant for sea-level operation (between points A and B). For flight in the stratosphere, outer-compressor efficiency increases from 0.85 to 0.87 between Mach 0.9 and 1.28 (points C and A), and decreases from 0.87 to 0.83 between Mach 1.28 and 2.32 (points A and D).

Figures 3(a), (b), and (c) show that the pressure-ratio split has little effect on the position of the operating line with respect to the outer-compressor stall-limit line. A more effective way to separate the two lines is to design the engine so that the outer-compressor design equivalent weight flow is higher than the outer-compressor reference-point equivalent weight flow.

The inner-compressor map of engines 20.7c and 20.9 is shown in figure 3(d). The operating line tends to parallel the stall-limit line, with the result that considerable margin between the two lines exists for the full range of flight conditions. Inner-compressor efficiency is practically constant at 0.87 for the full range of flight conditions. Inner-compressor maps for engines 20.7a and 20.7b are not shown because the full range of flight Mach number was unattainable.

Engines 15.7 and 15.9. - The outer- and inner-compressor maps of engines 15.7 and 15.9 are shown in figure 4. As with engines 20.7c and 20.9, the engine design weight flow (fig. 4(a)) was assigned to be 3 pounds per second greater than that at the outer-compressor reference point. The margin between the equilibrium operating line and the stall-limit line decreases as flight Mach number increases until, at Mach 2.32, the equivalent weight flow difference between the operating point and the stall-limit point is only 2.5 pounds per second. The outer-compressor efficiency is constant at 0.88 for all sea-level operation. For flight in the stratosphere, efficiency increases from 0.86 to 0.88 between Mach 0.9 and 1.28 (points C and A), and decreases from 0.88 to 0.86 between Mach 1.28 and 2.32 (points A and D).

The inner-compressor map of engines 15.7 and 15.9 is shown in figure 4(b). There is considerable margin between the equilibrium operating line and the inner-compressor stall-limit line. For the full range of flight conditions, efficiency is almost constant at 0.87.

Engines 9.7 and 9.9. - The outer- and inner-compressor maps of engines 9.7 and 9.9 are shown in figure 5. As with engines 20.7c, 20.9, 15.7, and 15.9, the outer-compressor design weight flow (fig. 5(a)) was assigned to be 3 pounds per second greater than the outer-compressor reference-point weight flow. The margin between the equilibrium operating line and the stall line decreases as flight Mach number increases, but even at Mach 2.32 the equivalent weight flow difference between the operating point and the stall-limit point is 8.2 pounds per second.

Therefore, stable operation over the full range of flight conditions would have resulted even if the outer-compressor design point and the outer-compressor reference point were made to coincide. At each equivalent speed $N_0/\sqrt{\theta_1}$, the outer compressor operates close to maximum efficiency. Over the full range of flight conditions considered, outer-compressor efficiency varies less than 2 percent.

The inner-compressor map of engines 9.7 and 9.9 is shown in figure 5(b). There is considerable margin between the equilibrium operating line and the inner-compressor stall-limit line. For sea-level operation, inner-compressor efficiency is constant at 0.88. For flight in the stratosphere, inner-compressor efficiency increases from 0.87 to 0.88 between Mach 0.9 and 1.28 (points C and A), and decreases from 0.88 to 0.85 between Mach 1.28 and 2.32 (points A and D).

Effect of design pressure ratio. - From figures 3(c), 4(a), and 5(a), it is seen that the margin between the outer-compressor equilibrium operating line and its stall-limit line is smallest at the highest flight Mach number and that the margin at the higher flight Mach numbers decreases as design compressor total-pressure ratio increases. The likelihood of surging the outer compressor is therefore greater at the higher flight Mach numbers, and this tendency becomes more pronounced as design compressor total-pressure ratio is increased. For the range of flight conditions considered, outer-compressor efficiency varies 4 percent for engines 20.7c and 20.9, and about 2 percent for engines 15.7, 15.9, 9.7, and 9.9.

Figures 3(d), 4(b), and 5(b) show that the margin between the inner-compressor equilibrium operating line and its stall-limit line is appreciable for the range of flight conditions considered; the effect of design compressor total-pressure ratio on this margin appears to be slight. The inner-compressor efficiency is practically constant for engines 20.7c, 20.9, 15.7, and 15.9, and varies only 3 percent for engines 9.7 and 9.9. Thus, this analysis indicates no serious problems with respect to the inner compressor.

Gas-Generator Performance

The gas-generator performance of engines 20.7c, 20.9, 15.7, 15.9, 9.7, and 9.9 is shown in figure 6. The variations of compressor-inlet equivalent weight flow $w_1\sqrt{\theta_1}/\delta_1$ (fig. 6(a)), compressor-exit equivalent weight flow $w_3\sqrt{\theta_3}/\delta_3$ (fig. 6(b)), compressor temperature ratio T_3/T_1 (fig. 6(c)), and engine temperature ratio T_6/T_1 (fig. 6(d)) with outer-compressor equivalent speed $N_0/\sqrt{\theta_1}$ for engines having a 30-percent total-pressure loss between the inner compressor and inner turbine are the same as those for the corresponding engines having a

10-percent total-pressure loss. Only the variation of engine pressure ratio P_6/P_1 (figs. 6(e) and (f)) is different for the two series of engines.

The differences in compressor-inlet equivalent weight flow (fig. 6(a)) among the engines are less than 1 percent at equivalent speeds above design. At equivalent speeds less than design, engines 9.7 and 9.9 pass more equivalent weight flow than engines 15.7, 15.9, 20.7c, and 20.9. At 80-percent outer-compressor equivalent speed (corresponding to a flight Mach number of 2.32 in the stratosphere), compressor-inlet equivalent weight flow for engines 9.7 and 9.9 is 8.5 percent larger than that for engines 15.7 and 15.9, and 13.8 percent larger than that for engines 20.7c and 20.9.

For a specified limiting Mach number in the duct downstream of the compressor exit, the flow area required is directly proportional to the compressor-exit equivalent weight flow. For each engine, compressor-exit equivalent weight flow (fig. 6(b)) increases as outer-compressor equivalent speed decreases. At 80-percent speed, compressor-exit equivalent weight flow (and, therefore, flow area) for engines 20.7c and 20.9 is about 22 percent less than that for engines 15.7 and 15.9, and 50 percent less than that for engines 9.7 and 9.9.

The compressor temperature ratio T_3/T_1 (fig. 6(c)) of each engine increases with outer-compressor equivalent speed. At each equivalent speed, compressor temperature ratio increases with design compressor pressure ratio. The engine temperature ratio T_6/T_1 (fig. 6(d)) of each engine increases with outer-compressor equivalent speed, but it decreases with design compressor pressure ratio at each equivalent speed.

The engine pressure ratio P_6/P_1 (figs. 6(e) and (f)) of each engine increases with outer-compressor equivalent speed. At 80-percent speed (fig. 6(e)), the highest engine pressure ratio is achieved by engine 9.7; whereas at 110 percent speed, the highest value is achieved by engine 15.7. The engine-pressure-ratio variations for engines 20.9, 15.9, and 9.9 (fig. 6(f)) are similar to those for engines 20.7, 15.7, and 9.7 (fig. 6(e)). At each speed, the engine-pressure-ratio value from figure 6(f) is 9/7 of the corresponding value from figure 6(e).

Engine Performance

Comparison of engines 20.7a, 20.7b, and 20.7c. - The performances of engines 20.7a, 20.7b, and 20.7c with the afterburner inoperative are shown in figure 7. Equivalent net thrust is plotted against flight Mach number in figure 7(a). At sea level, flight Mach number is varied from

0 to 0.9. In the stratosphere, flight Mach number is varied from 0.9 to 2.32 for engine 20.7c. Because the operating line on the outer-compressor map intersects the stall-limit line, the maximum flight Mach numbers for engines 20.7a and 20.7b are 1.925 and 1.972, respectively. The thrust values for engines 20.7a and 20.7b are within 2 percent of one another. The variation in thrust among the three engines is 2 percent or less for flight Mach numbers less than 0.7 at sea level and for Mach numbers less than 1.5 in the stratosphere. At Mach 0.9 sea level, the thrust for engine 20.7c is about 5 percent higher than that for engine 20.7a; and at Mach 1.92 in the stratosphere, the thrust of engine 20.7c is about 6 percent higher than that for engine 20.7a.

Specific power for the three engines is plotted against flight Mach number in figure 7(b). The maximum difference in specific power between engines 20.7a and 20.7b is less than 1 percent. Over part of the flight range, the specific-power values for engine 20.7c are lower than those for engines 20.7a and 20.7b. The maximum variation occurs at Mach 1.92 in the stratosphere, where the specific power for engine 20.7c is about 2 percent lower than that for engine 20.7b.

Comparison of engines 20.7c, 15.7, and 9.7. - The performances of engines 20.7c, 15.7, and 9.7 with the afterburner inoperative are shown in figure 8. At any flight Mach number (fig. 8(a)), thrust increases as design compressor pressure ratio decreases. At Mach 0.9 at sea level, the thrust for engine 9.7 is about 10 percent greater than that for engine 15.7, and about 18 percent greater than that for engine 20.7c. In the stratosphere, each engine attains its maximum equivalent net thrust at a different flight Mach number: For engine 9.7, it is Mach 2.32; for engine 15.7, 1.95; and for engine 20.7c, 1.65. The maximum equivalent net thrust for engine 9.7 is about 29 percent greater than that for engine 15.7, and 47 percent greater than that for engine 20.7c.

Over the flight range up to Mach 2.0, specific power (fig. 8(b)) decreases as design compressor pressure ratio increases. At Mach 0.9 at sea level, the specific power for engine 20.7c is about 6 percent less than that for engine 15.7, and 18 percent less than that for engine 9.7. At Mach 2.32 in the stratosphere, the specific-power values for engines 9.7 and 20.7c are the same, but that for engine 15.7 is about 4 percent less.

The performances of engines 20.7c, 15.7, and 9.7 with chemical afterburning at 3500° R are shown in figure 9. At sea level, the equivalent net thrust values (fig. 9(a)) of engines 20.7c and 15.7 are the same. Thrust for these engines is 1 to 5 percent greater than that for engine 9.7. In the stratosphere up to Mach 1.6, the thrust values of engines 20.7c and 15.7 are the same, and are greater than those for engine 9.7 by 5 percent or less. Above Mach 1.6, thrust increases as

design compressor pressure ratio decreases. At Mach 2.32, the thrust for engine 9.9 is about 8 percent greater than that for engine 15.9, and 18 percent greater than that for engine 20.9.

Specific power for operation with afterburning at 3500° F (fig. 9(b)) decreases as design compressor pressure ratio increases. In the stratosphere, specific power decreases as flight Mach number increases. The reverse is true when the afterburner is inoperative (fig. 8(b)). At Mach 0.9 at sea level, specific power for engine 20.7c (fig. 9(b)) is about 13 percent less than that for engine 15.7, and 30 percent less than that for engine 9.7. At Mach 2.32 in the stratosphere, specific power for engine 20.7c is about 22 percent less than that for engine 15.7, and 40 percent less than that for engine 9.7.

Specific fuel consumption for operation with afterburning at 3500° R is plotted against flight Mach number in figure 9(c). For each engine, specific fuel consumption increases with flight Mach number. At any flight Mach number, specific fuel consumption increases with design compressor pressure ratio. At Mach 0.9 at sea level, specific fuel consumption for engine 9.7 is about 4 percent less than that for engine 15.7, and 10 percent less than that for engine 20.7c. At Mach 2.32 in the stratosphere, the advantage for engine 9.7 over engines 15.7 and 20.7c is about 8 and 16 percent, respectively.

Comparison of engines 20.9, 15.9, and 9.9. - The trends exhibited by the engines having a 10-percent pressure drop between the inner compressor and inner turbine are similar to those of the engines having a 30-percent pressure drop. The performance of engines 20.9, 15.9, and 9.9 with the afterburner inoperative is shown in figure 10. At any flight Mach number (fig. 10(a)), thrust increases as design compressor pressure ratio decreases. At Mach 0.9 at sea level, thrust for engine 9.9 is about 9 percent greater than that for engine 15.9, and 18 percent greater than that for engine 20.9. In the stratosphere, each engine attains its maximum equivalent net thrust at a different flight Mach number: For engine 9.9, it is Mach 2.32; for engine 15.9, 2.1; and for engine 20.9, 1.7. The maximum equivalent net thrust for engine 9.9 is about 30 percent greater than that for engine 15.9, and 51 percent greater than that for engine 20.9.

At any flight Mach number, specific power (fig. 10(b)) decreases as design compressor pressure ratio increases. At Mach 0.9 at sea level, the specific power for engine 20.9 is about 7 percent less than that for engine 15.9, and 18 percent less than that for engine 9.7. At Mach 2.32 in the stratosphere, the advantage in specific power for engine 20.9 over engines 15.9 and 9.9 is 0.4 and 7 percent, respectively.

The performances of engines 20.9, 15.9, and 9.9 with afterburning at 3500° R are shown in figure 11. At sea level, the equivalent net

thrust (fig. 11(a)) of engines 15.9 and 20.9 is approximately the same, and higher than that for engine 9.9 by 7 percent or less. In the stratosphere up to Mach 1.6, the thrust values of engines 20.9 and 15.7 are about the same, and they are greater than those of engine 9.9 by 4 percent or less. Above Mach 1.6, thrust increases as design compressor pressure ratio decreases. At Mach 2.32, the thrust for engine 9.9 is about 8 percent greater than that for engine 15.9, and 18 percent greater than that for engine 20.9.

Specific power for operation with afterburning at 3500° R (fig. 11(b)) decreases as design compressor pressure ratio increases. At Mach 0.9 at sea level, specific power for engine 20.9 is about 20 percent less than that for engine 15.9, and 31 percent less than that for engine 9.9. At Mach 2.32 in the stratosphere, specific power for engine 20.9 is about 25 percent less than that for engine 15.9, and 41 percent less than that for engine 9.9.

Specific fuel consumption for operation with afterburning at 3500° R is plotted against flight Mach number in figure 11(c). For each engine, specific fuel consumption increases with flight Mach number. At any flight Mach number, specific fuel consumption increases with design compressor pressure ratio. At Mach 0.9 at sea level, specific fuel consumption for engine 9.9 is about 11 percent less than that for engine 15.9, and 16 percent less than that for engine 20.9. At Mach 2.32 in the stratosphere, the advantage for engine 9.9 over engines 15.9 and 20.9 is about 8 and 16 percent, respectively.

Effect of total-pressure loss between inner compressor and turbine. -
The effect of total-pressure loss between the inner-spool compressor and turbine on engine performance is presented as ratios of performance values of the engines with 10-percent pressure loss to those of engines with 30-percent loss.

The effect of total-pressure loss on the performance of engines with a design compressor pressure ratio of 20 is shown in the following table:

Altitude	M ₀	Ratio of value for engine <u>20.9</u> to value for engine <u>20.7c</u>				
		With afterburner inoperative		With afterburning at 3500° R		
		Thrust	Specific power	Thrust	Specific power	Specific fuel consumption
Sea level	0	1.136	0.880	1.143	0.874	0.875
Sea level	.9	1.174	.838	1.128	.872	.873
Stratosphere	.9	1.100	.910	1.087	.920	.920
Stratosphere	2.32	1.207	.828	1.080	.926	.927

With the afterburner inoperative, decreasing the total-pressure loss from 30 to 10 percent increases the thrust 10 to 21 percent and decreases the specific power 9 to 17 percent. For operation with afterburning, thrust increases 8 to 14 percent, specific power decreases 7 to 13 percent, and specific fuel consumption decreases 7 to 13 percent.

The effect of total-pressure loss on the performance of engines with a design compressor pressure ratio of 15 is shown in the following table:

Altitude	M_0	Ratio of value for engine <u>15.9</u> to value for engine <u>15.7</u>				
		With afterburner inoperative		With afterburning at 3500° R		
		Thrust	Specific power	Thrust	Specific power	Specific fuel consumption
Sea level	0	1.135	0.881	1.143	0.875	0.875
Sea level	.9	1.190	.841	1.150	.870	.870
Stratosphere	.9	1.096	.910	1.085	.920	.920
Stratosphere	2.32	1.163	.864	1.079	.922	.930

With the afterburner inoperative, decreasing the total-pressure loss from 30 to 10 percent increases the thrust 10 to 19 percent and decreases the specific power 9 to 17 percent. For operation with afterburning, thrust increases 8 to 15 percent, specific power decreases 8 to 13 percent, and specific fuel consumption decreases 8 to 13 percent.

The effect of total-pressure loss on the performance of engines with a design compressor pressure ratio of 9 is shown in the following table:

Altitude	M_0	Ratio of value for engine <u>9.9</u> to value for engine <u>9.7</u>				
		With afterburner inoperative		With afterburning at 3500° R		
		Thrust	Specific power	Thrust	Specific power	Specific fuel consumption
Sea level	0	1.151	0.869	1.158	0.864	0.863
Sea level	.9	1.185	.841	1.151	.866	.866
Stratosphere	.9	1.100	.906	1.089	.915	.915
Stratosphere	2.32	1.128	1.894	1.077	.938	.933

With the afterburner inoperative, decreasing the total-pressure loss from 30 to 10 percent increases the thrust 10 to 19 percent and decreases the specific power to 16 percent. For operation with afterburning, thrust increases 8 to 16 percent, specific power decreases 6 to 14 percent, and specific fuel consumption decreases 7 to 14 percent.

Summary Remarks

In this section, some observations are made concerning the engine surge problem at high flight Mach numbers and the trends in engine performance as design compressor pressure ratio increases. In addition, comparisons are made among engines sized to produce a particular thrust at a specified flight condition.

For engine operation at constant values of outer-compressor mechanical speed and inner-turbine inlet temperature, the outer-compressor operating point moves toward its stall-limit line as flight Mach number increases. In two of the engines with a design compressor total-pressure ratio of 20, the equilibrium operating line intersected the outer-compressor stall-limit line so that an engine surge problem existed. Varying the pressure-ratio split between the outer and inner compressors offered no solution. The problem was solved, however, by assigning the outer-compressor equivalent weight flow for the engine design point to be higher than that for outer-compressor peak efficiency.

From the engine performance curves (figs. 8 to 11) and the gas-generator curve of compressor-exit equivalent weight flow (fig. 6(b)), some general trends concerning the effect of design compressor pressure ratio are noted. With the afterburner inoperative, as design compressor pressure ratio increases, both thrust and specific power decrease. (An exception is the variation of specific power at flight Mach numbers above 2 for engines having a 30-percent pressure loss between the inner compressor and turbine.) For operation with chemical afterburning at 3500° R, as design compressor pressure ratio increases, thrust decreases for flight Mach numbers greater than 1.6, specific power decreases, and specific fuel consumption increases. For either type operation, as design compressor pressure ratio increases, compressor-exit equivalent weight flow decreases. Hence, the size of the ducts downstream of the compressor exit would decrease as would also the reactor size in the direct-air-cycle type of engine.

The magnitude of the compromises involved by selecting a design compressor pressure ratio is illustrated in the following two examples for engines having a 30-percent total-pressure loss between the inner compressor and turbine. Suppose that a specific value of thrust is required with the afterburner inoperative at a flight Mach number of 1.5.

Because the thrust per unit design weight flow decreases as design compressor pressure ratio increases, the design compressor weight flow would have to be about 9 percent greater for engine 15.7 and 17 percent greater for engine 20.7c than for engine 9.7. Thus, the weight of the compressors and turbines increases with design compressor pressure ratio for two reasons: (1) the number of compressor and turbine stages increases and (2) the frontal area of the compressor increases. The reactor power required at Mach 1.5 is 10 percent less for engine 15.7 and 15 percent less for engine 20.7c than for engine 9.7. Although the design compressor-inlet equivalent weight flow increases with design compressor pressure ratio, the compressor-exit equivalent weight flow per unit design compressor weight flow decreases; the latter effect predominates so that smaller ducts downstream of the compressor are required for the higher-pressure-ratio engines. The duct flow area is about 30 percent less for engine 15.7 and 41 percent less for engine 20.7c than for engine 9.7. Thus, the size of the reactor decreases as design compressor pressure ratio increases for two reasons: (1) the reactor power decreases, and (2) the duct size decreases.

As another example, suppose a specific value of thrust is required for operation with afterburning at a flight Mach number of 2.0 in the stratosphere. For such conditions, the design compressor weight flow would have to be about 5 percent greater for engine 15.7 and 11 percent greater for engine 20.7c than for engine 9.7. The reactor power would be 21 percent less for engine 15.7 and 34 percent less for engine 20.7 than for engine 9.7. The duct flow area downstream of the compressor would be about 33 percent less for engine 15.7 and 45 percent less for engine 20.7c than for engine 9.7.

SUMMARY OF RESULTS

The following results were obtained from an analytical investigation to compare the performance of hypothetical two-spool turbojets having design compressor total-pressure ratios of 20, 15, and 9 and total-pressure losses between the inner compressor and inner turbine of 10 and 30 percent. Each engine operates with the outer-compressor mechanical speed fixed at its design value and the inner-turbine inlet temperature fixed at 2160° R. Performance with chemical afterburning at 3500° R and with the afterburner inoperative was calculated for flight Mach numbers of 0 to 0.9 at sea level and 0.9 to 2.32 in the stratosphere. An engine is referred to by its design value of compressor total-pressure ratio.

1. For engines having a 10-percent pressure loss and operating with the afterburner inoperative, the maximum equivalent net thrust for engine 9 is about 30 percent greater than that for engine 15, and 51 percent greater than that for engine 20. At each flight Mach number, specific power decreases as design compressor pressure ratio increases.

2. At Mach 2.32, the engines having a 10-percent pressure loss and operating with afterburning perform as follows: Thrust for engine 9 is about 8 percent greater than that for engine 15, and 18 percent greater than that for engine 20. Specific power for engine 20 is about 25 percent less than that for engine 15, and 41 percent less than that for engine 9. Specific fuel consumption for engine 9 is about 8 percent less than that for engine 15, and 16 percent less than that for engine 20.

3. For engines having a 30-percent pressure loss and operating with the afterburner inoperative, the maximum equivalent net thrust for engine 9 is about 29 percent greater than that for engine 15, and 47 percent greater than that for engine 20. Below Mach 2.0, specific power decreases as design compressor pressure ratio increases. At Mach 2.32, the specific-power values for engines 9 and 20 are the same, whereas that for engine 15 is about 4 percent less.

4. Engines with a 30-percent pressure loss and operating with afterburning have the following performance at Mach 2.32: Thrust for engine 9 is greater than that for engines 15 and 20 by about 8 and 18 percent, respectively. Specific power for engine 20 is less than that for engines 15 and 9 by about 22 and 41 percent, respectively. Specific fuel consumption for engine 9 is less than that for engines 15 and 20 by about 8 and 16 percent, respectively.

5. At Mach 2.32, the flow area downstream of the compressor exit for engine 20 is less than that for engines 15 and 9 by about 21 and 50 percent, respectively.

6. The possibility of surging the outer compressor is greater at the lower equivalent speeds than at the higher speeds. This tendency becomes more pronounced as design compressor pressure ratio is increased.

7. The design pressure-ratio split between the outer and the inner compressor has little effect on engine performance or on the outer-compressor surge problem. Margin between the operating line and the outer-compressor stall-limit line can be attained by assigning the outer-compressor design-point equivalent weight flow to be higher than that for outer-compressor peak efficiency.

8. For operation with the afterburner inoperative, decreasing the total-pressure loss from 30 to 10 percent increases the thrust 10 to 21 percent and decreases the specific power 9 to 17 percent. For operation with chemical afterburning at 3500° R, thrust increases 8 to 16 percent, specific power decreases 6 to 14 percent, and specific fuel consumption decreases 7 to 14 percent.

APPENDIX - SYMBOLS

C_v	velocity coefficient
c_p	specific heat at constant pressure, Btu/(lb)($^{\circ}$ R)
F	thrust, lb
f	fuel-air ratio
g	standard gravitational acceleration, 32.174 ft/sec ²
H	total enthalpy, Btu/lb
M	Mach number
N	rotational speed, rpm
P	total pressure, lb/sq ft
p	static pressure, lb/sq ft
R	gas constant, 35.345 ft-lb/(lb)($^{\circ}$ R)
sfc	specific fuel consumption, lb fuel/(hr)(lb thrust)
sp	specific power, kw/lb thrust
T	total temperature, $^{\circ}$ R
t	static temperature, $^{\circ}$ R
V	velocity, ft/sec
w	weight flow, lb/sec
γ	ratio of specific heat at constant pressure to specific heat at constant volume
δ	ratio of total pressure to NACA standard sea-level pressure, $P/2116$
η	adiabatic efficiency
θ	ratio of total temperature to NACA standard sea-level temperature, $T/518.7$

Subscripts:

c compressor
d design
i inner spool
j jet
n net
o outer spool
0 ambient conditions
1 outer-compressor inlet
2 inner-compressor inlet
3 inner-compressor exit
4 inner-turbine inlet
5 outer-turbine inlet
6 outer-turbine exit
7 exhaust-nozzle inlet

REFERENCES

1. Dugan, James F., Jr.: Effect of Design Over-All Compressor Pressure Ratio Division on Two-Spool Turbojet-Engine Performance and Geometry. NACA RM E54F24a, 1954.
2. Dugan, James F., Jr.: Performance and Component Frontal Areas of a Hypothetical Two-Spool Turbojet Engine for Three Modes of Operation. NACA RM E55H31, 1955.
3. Turner, L. Richard, and Bogart, Donald: Constant-Pressure Combustion Charts Including Effects of Diluent Addition. NACA Rep. 937, 1949. (Supersedes NACA TN's 1086 and 1655.)
4. Keenan, Joseph H., and Kaye, Joseph: Gas Tables. John Wiley & Sons, Inc., 1948.

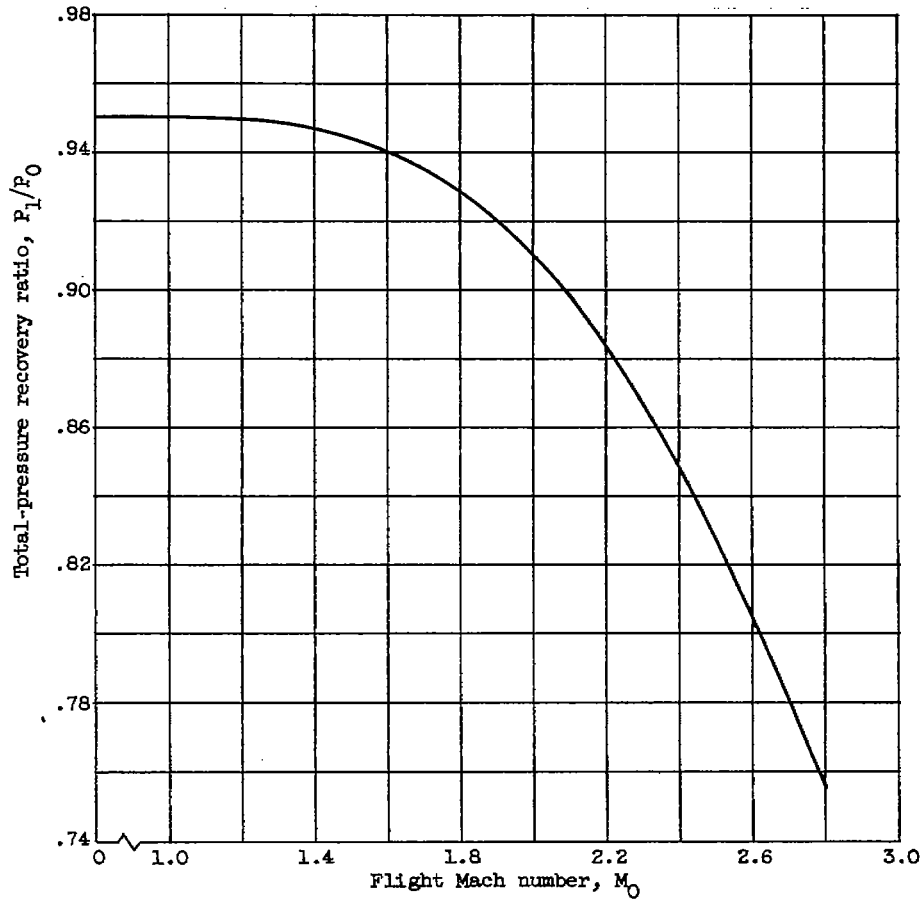


Figure 1. - Performance of inlet with two adjustable wedges.

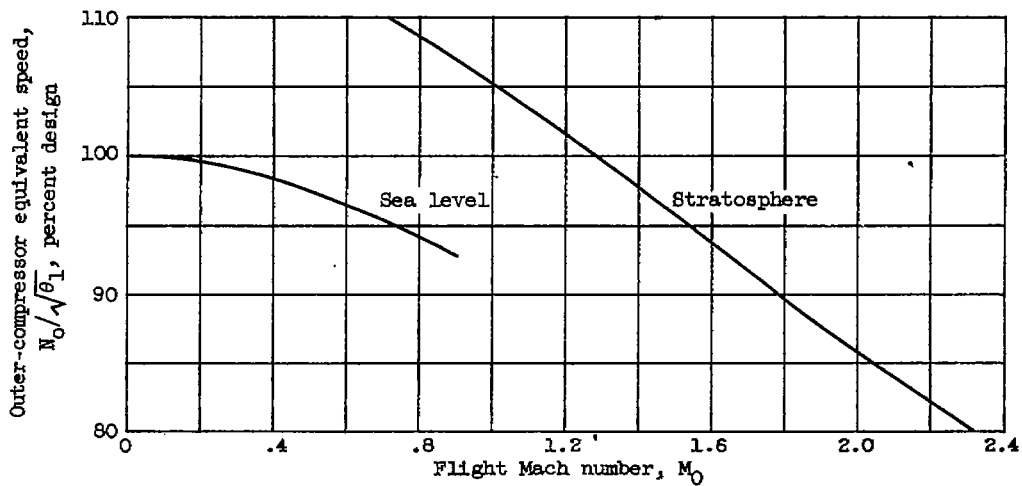
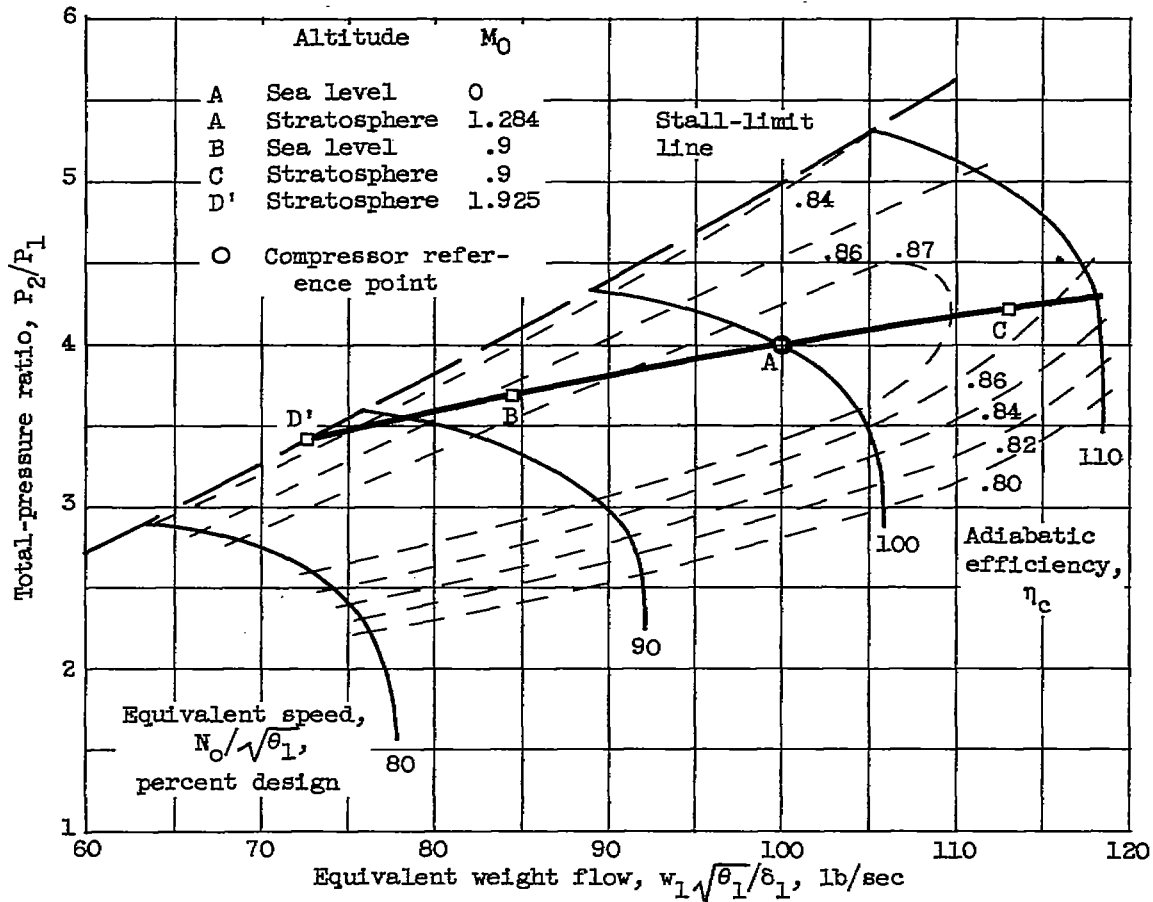


Figure 2. - Variation of outer-compressor equivalent speed with flight condition for operation with outer-compressor mechanical speed maintained constant at its design value.



(a) Outer-compressor map of engine 20.7a.

Figure 3. - Compressor maps of engines 20.7a, 20.7b, 20.7c, and 20.9.

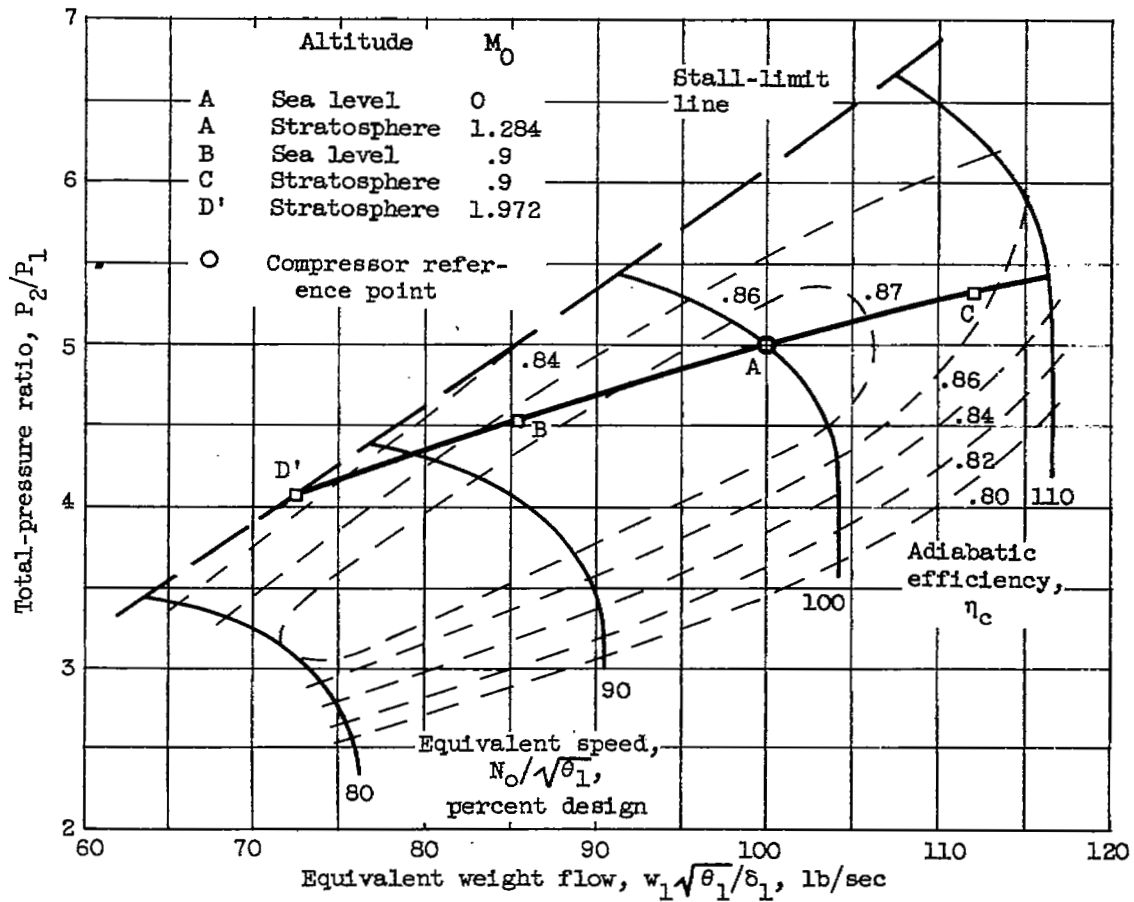
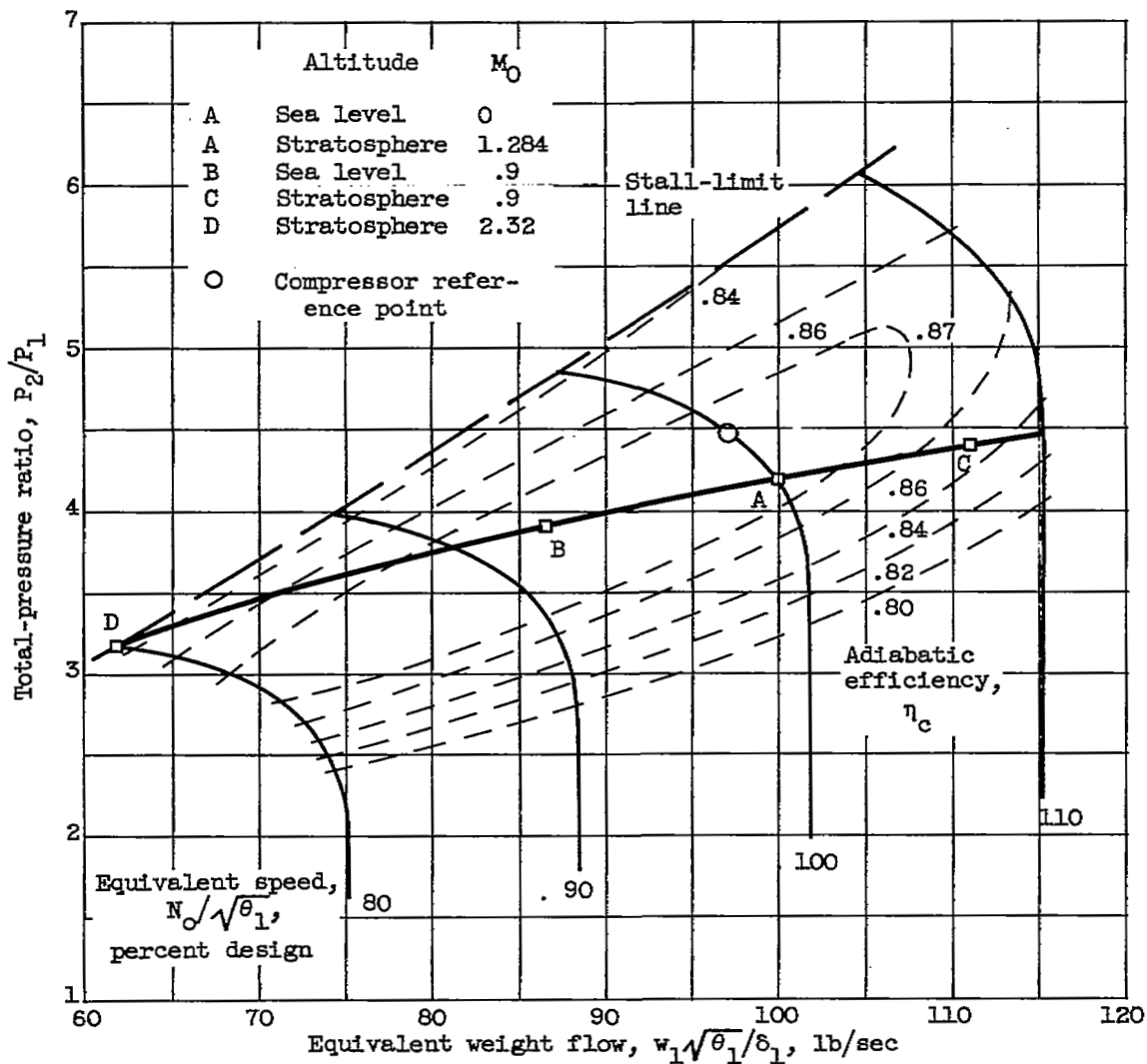
(b) Outer-compressor map of engine 20.7b.

Figure 3. - Continued. Compressor maps of engines 20.7a, 20.7b, 20.7c, and 20.9.



(c) Outer-compressor map of engines 20.7c and 20.9.

Figure 3. - Continued. Compressor maps of engines 20.7a, 20.7b, 20.7c, and 20.9.

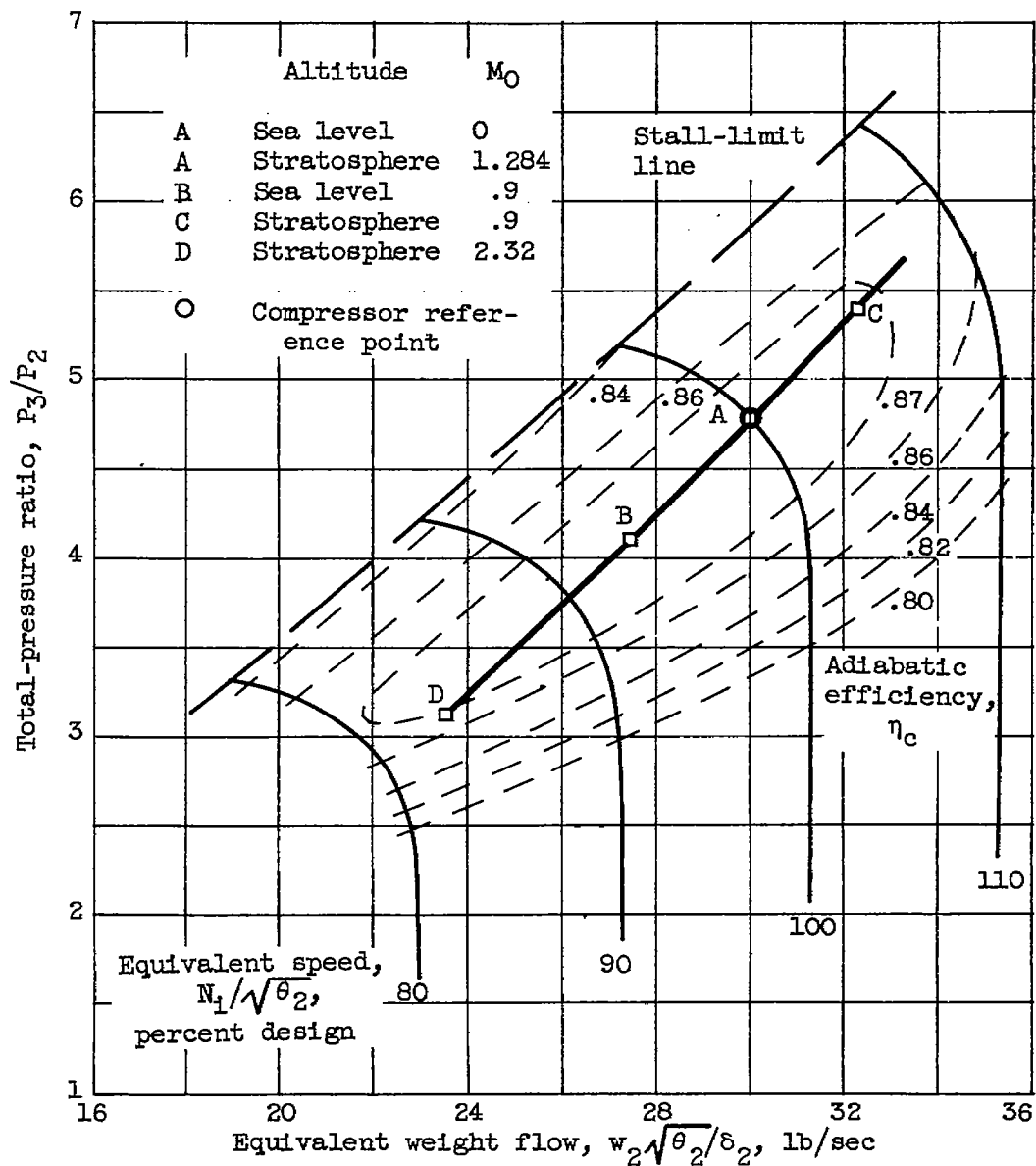
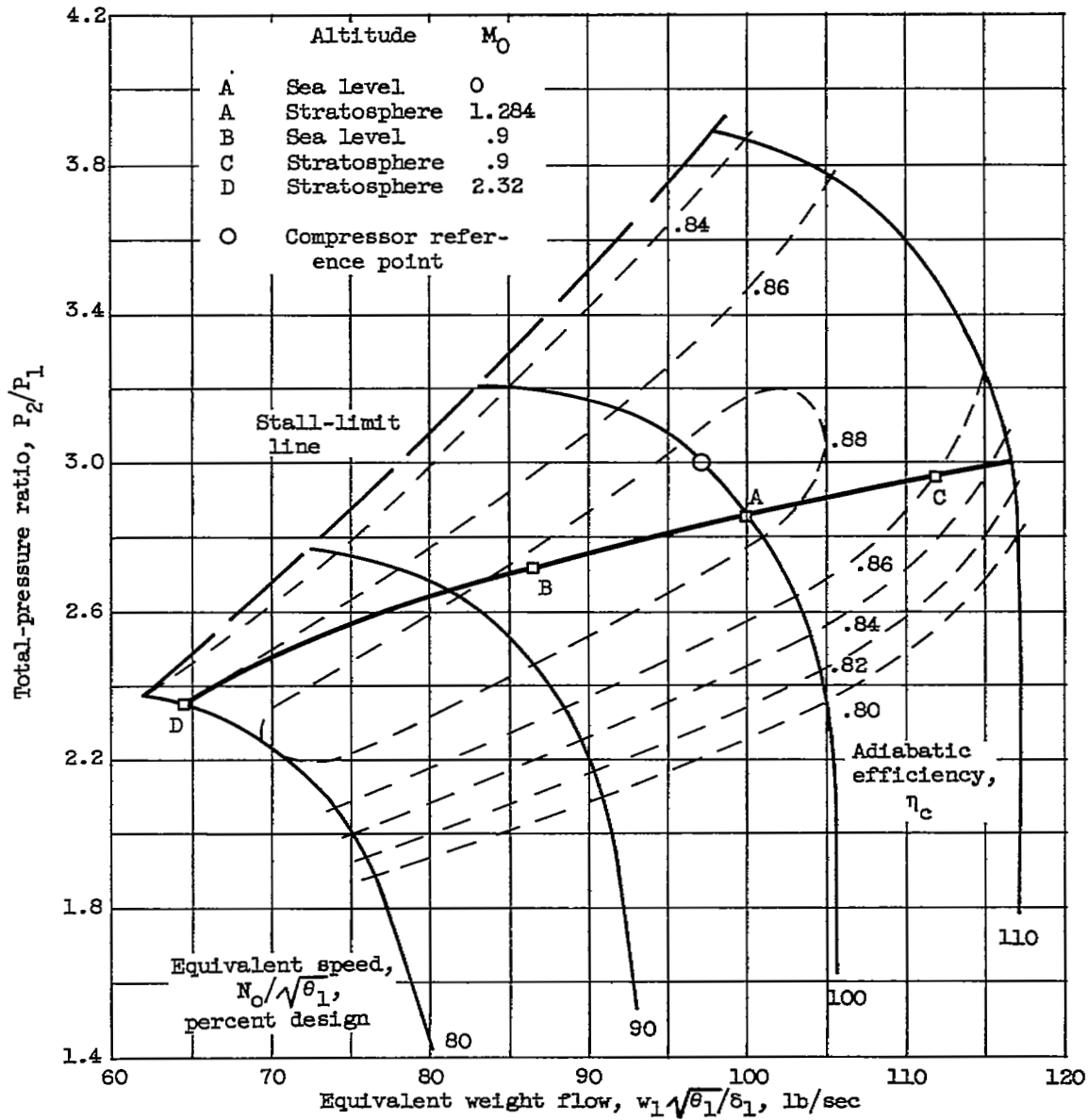
(d) Inner-compressor map of engines 20.7c and 20.9.

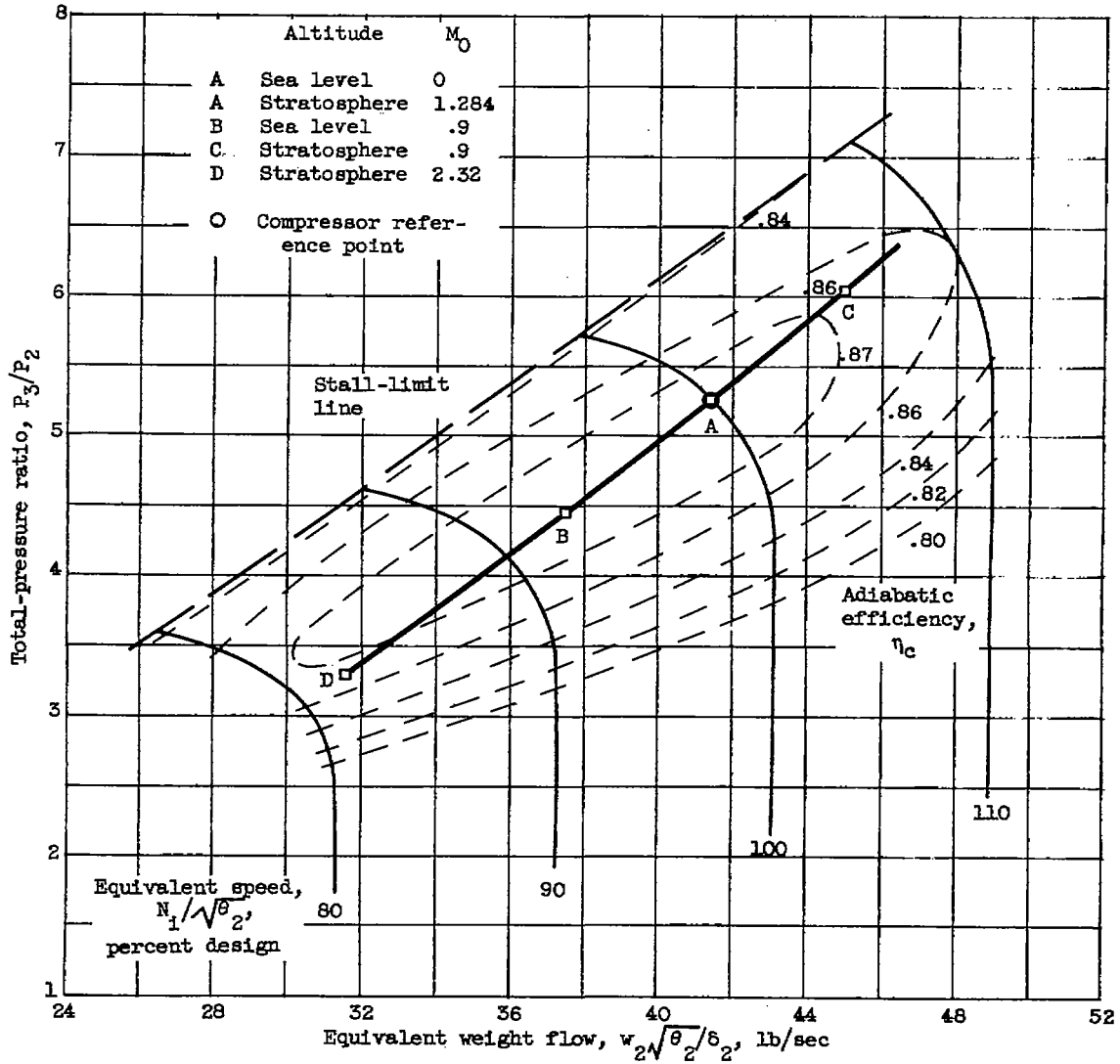
Figure 3. - Concluded. Compressor maps of engines 20.7a, 20.7b, 20.7c, and 20.9.

3909



(a) Outer compressor.

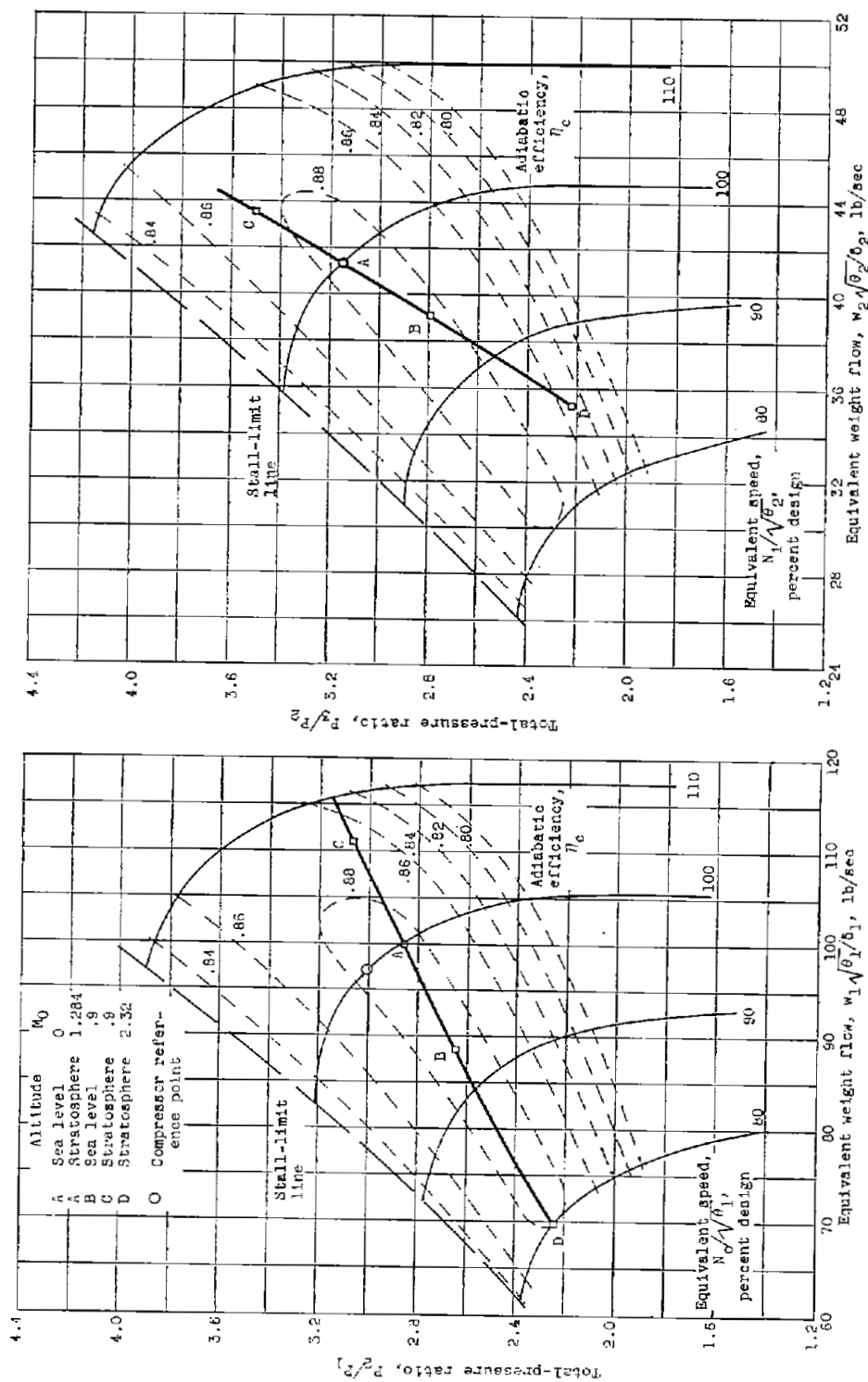
Figure 4. - Compressor maps of engines 15.7 and 15.9.



(b) Inner compressor.

Figure 4. - Concluded. Compressor maps of engines 15.7 and 15.9.

3909



(a) Outer compressor.

(b) Inner compressor.

Figure 5. - Compressor maps of engines 9.7 and 9.3.

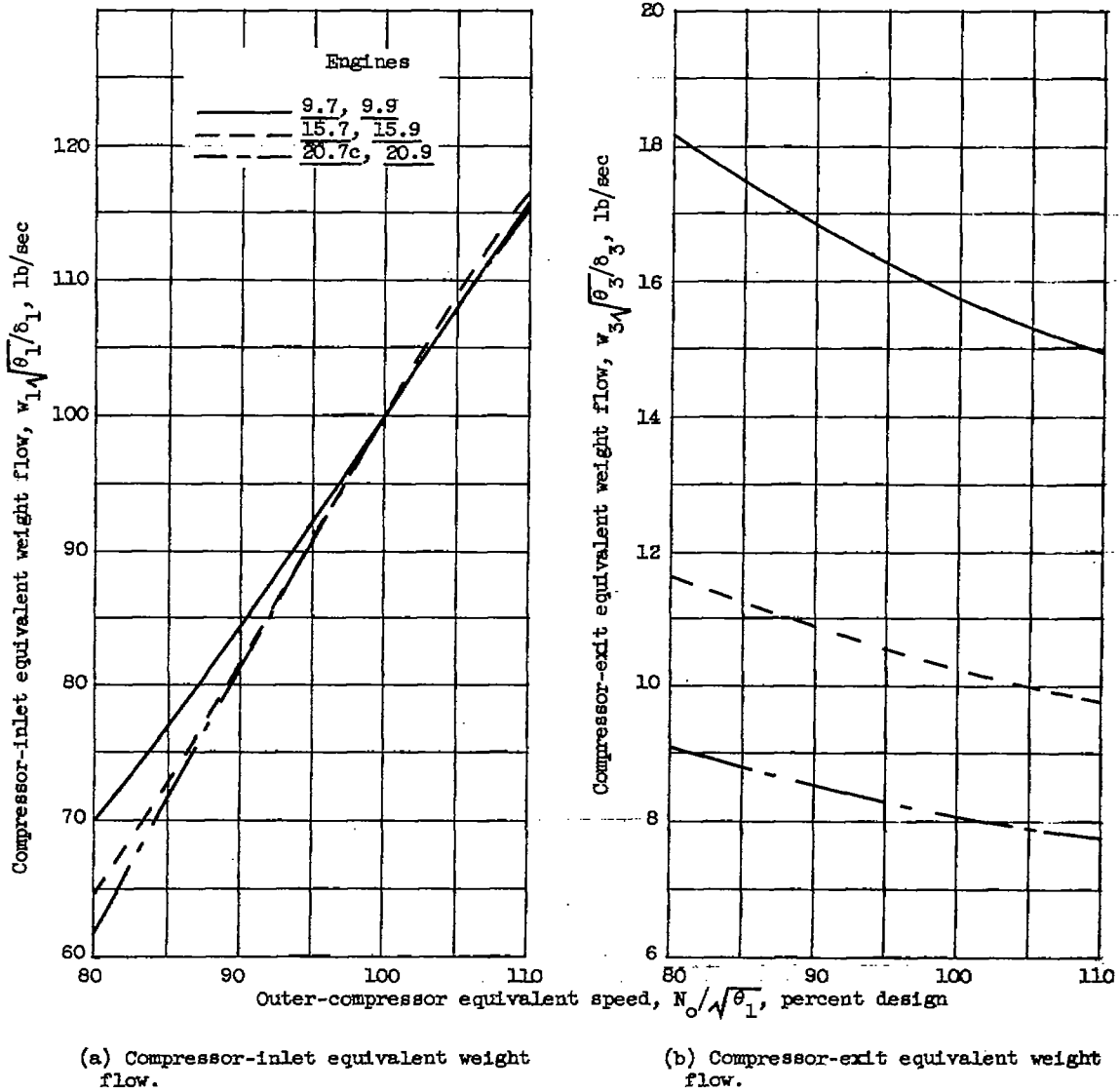
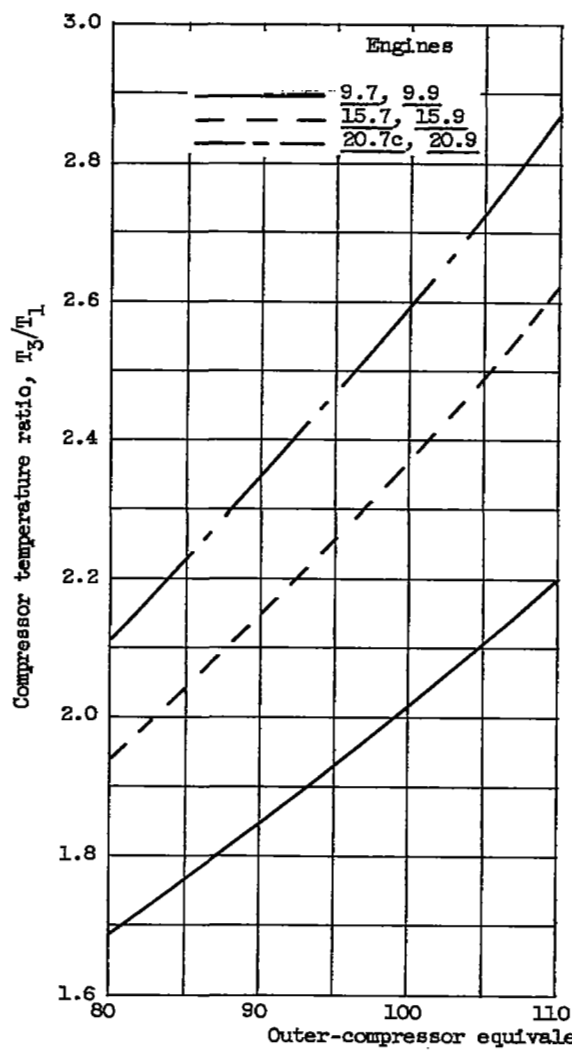
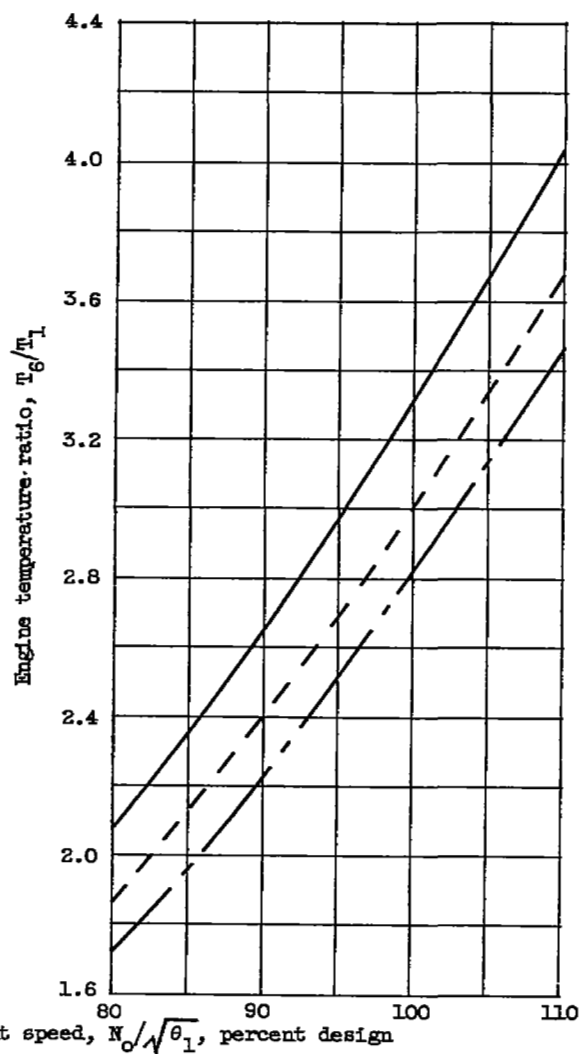


Figure 6. - Gas-generator performance.

CP-5
3909

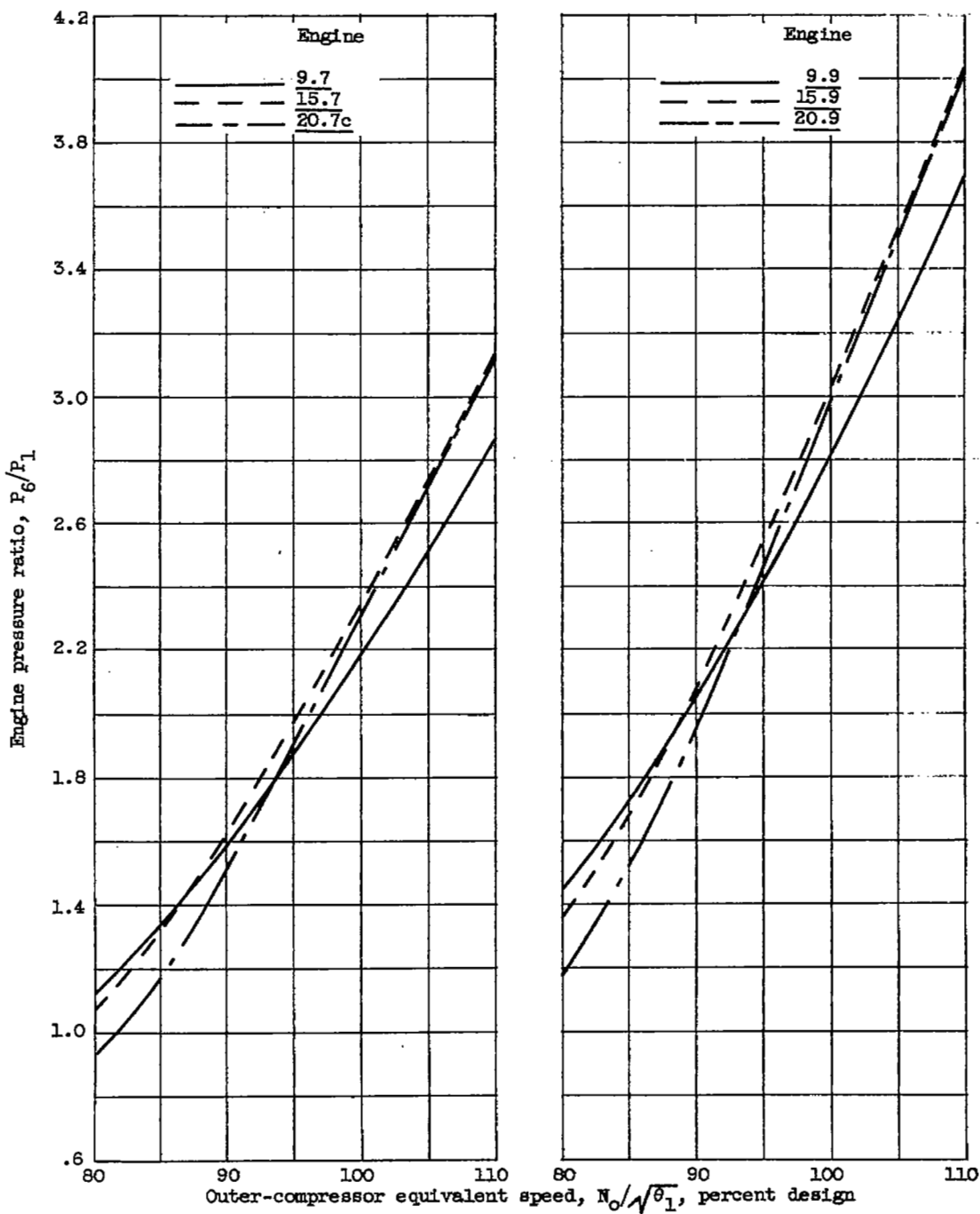


(c) Compressor temperature ratio.



(d) Engine temperature ratio.

Figure 6. - Continued. Gas-generator performance.

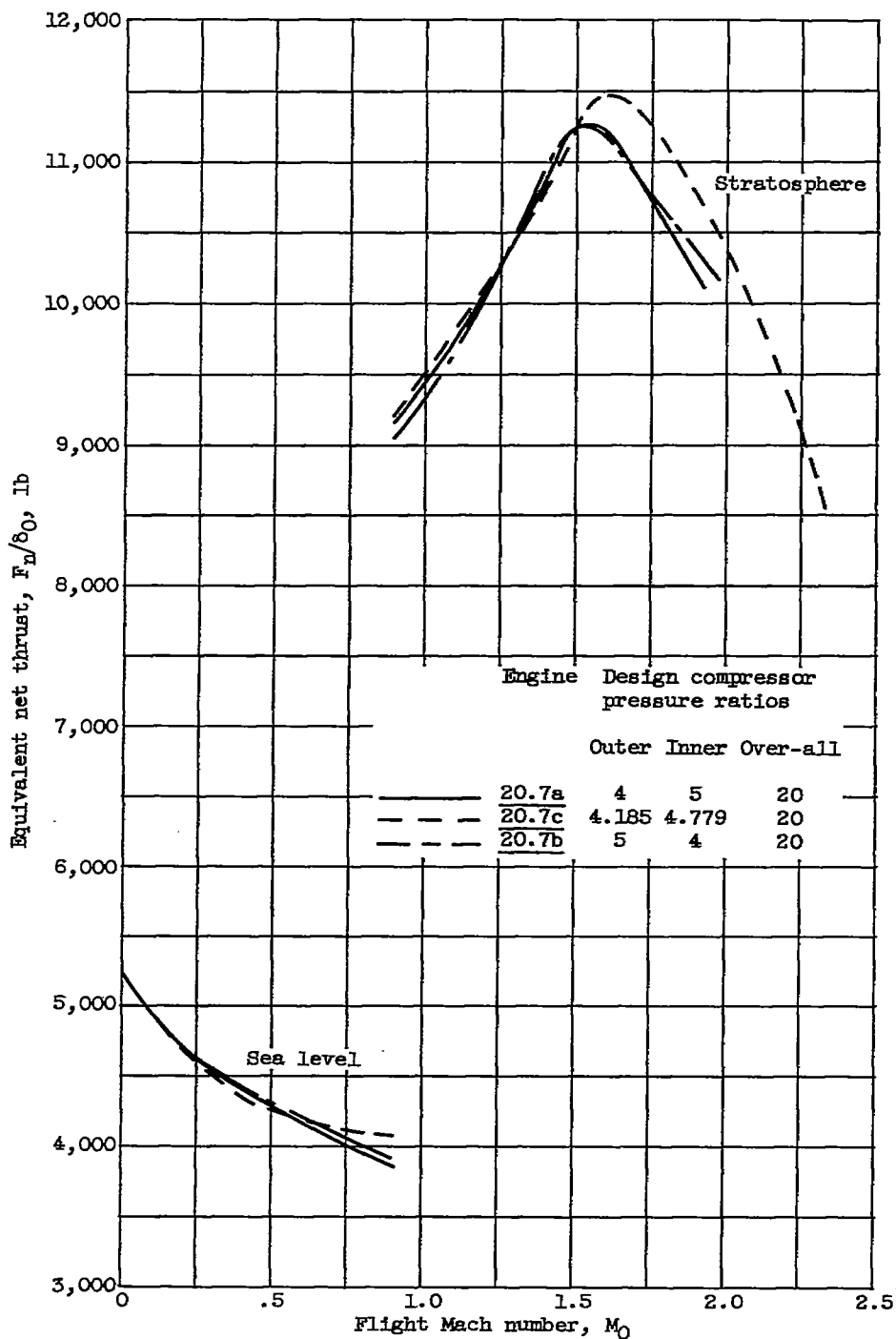


(e) Engine pressure ratio, with 30-percent inner-spool total-pressure loss.

(f) Engine pressure ratio, with 10-percent inner-spool total-pressure loss.

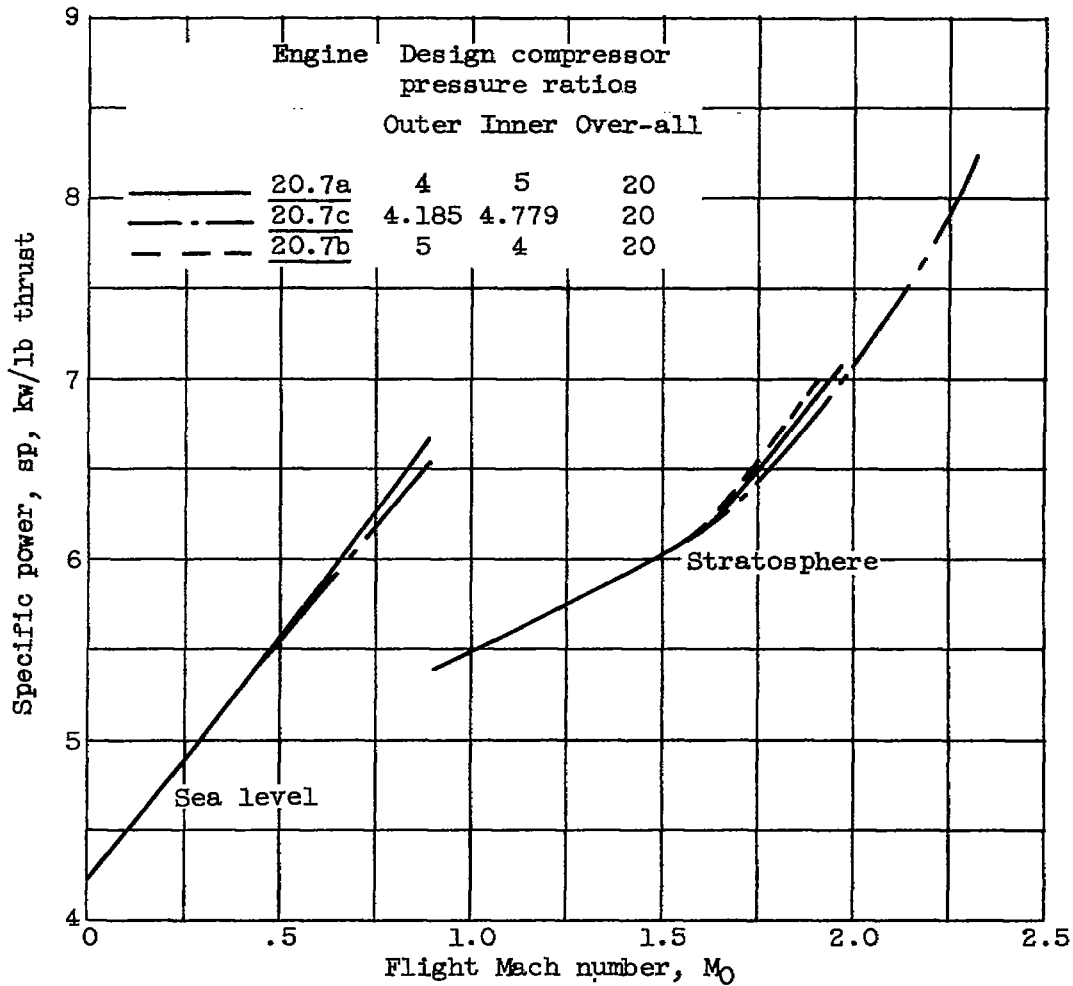
Figure 6. - Concluded. Gas-generator performance.

CP-5 back 3909



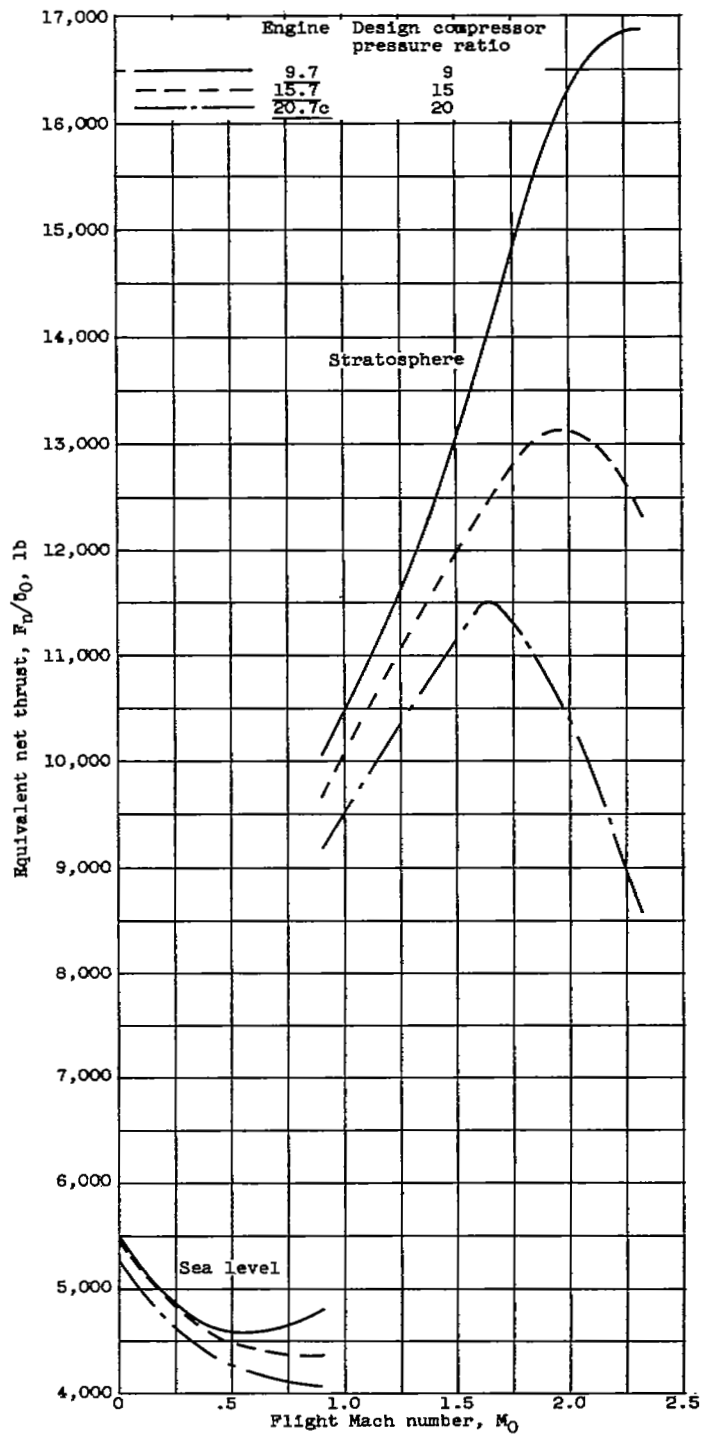
(a) Equivalent net thrust.

Figure 7. - Performance of engines 20.7a, 20.7b, and 20.7c with afterburner inoperative.



(b) Specific power.

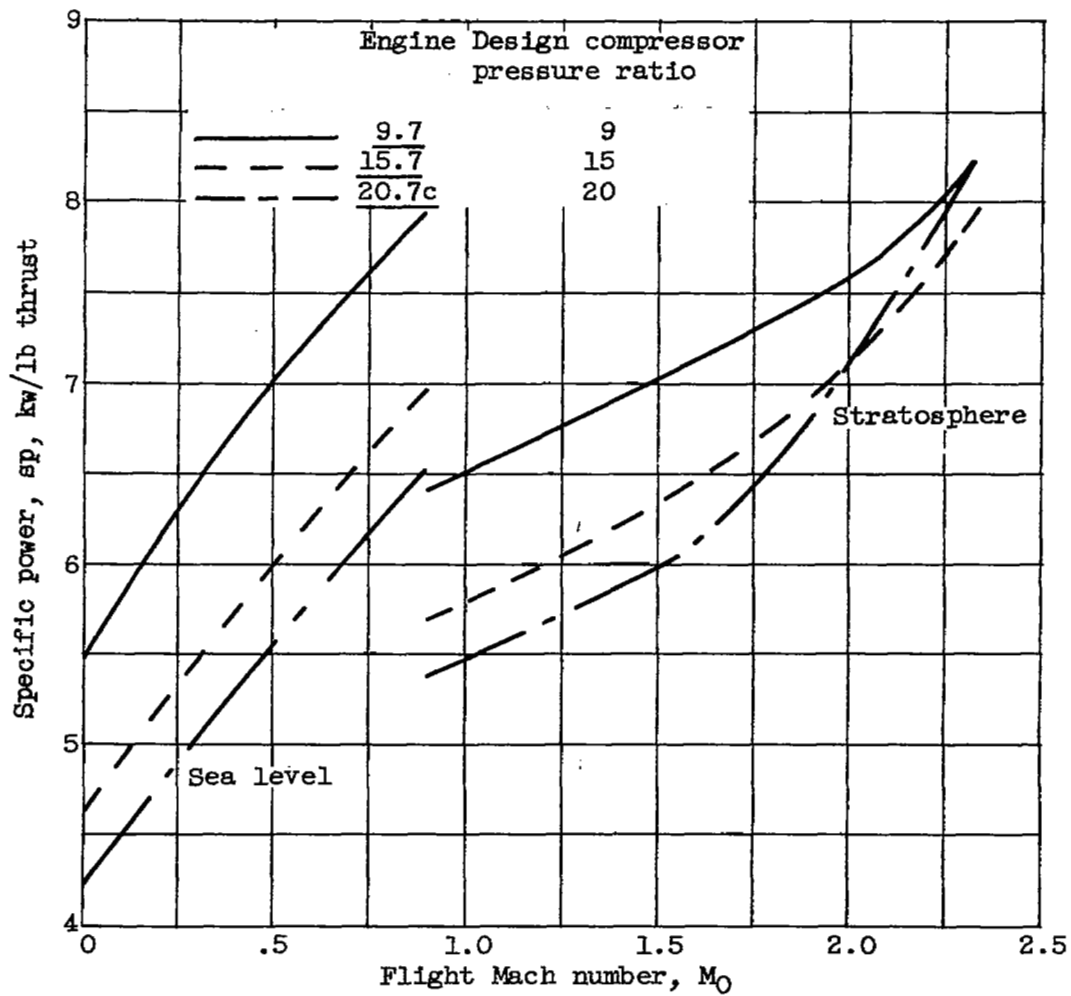
Figure 7. - Concluded. Performance of engines 20.7a, 20.7b, and 20.7c with afterburner inoperative.



(a) Equivalent net thrust.

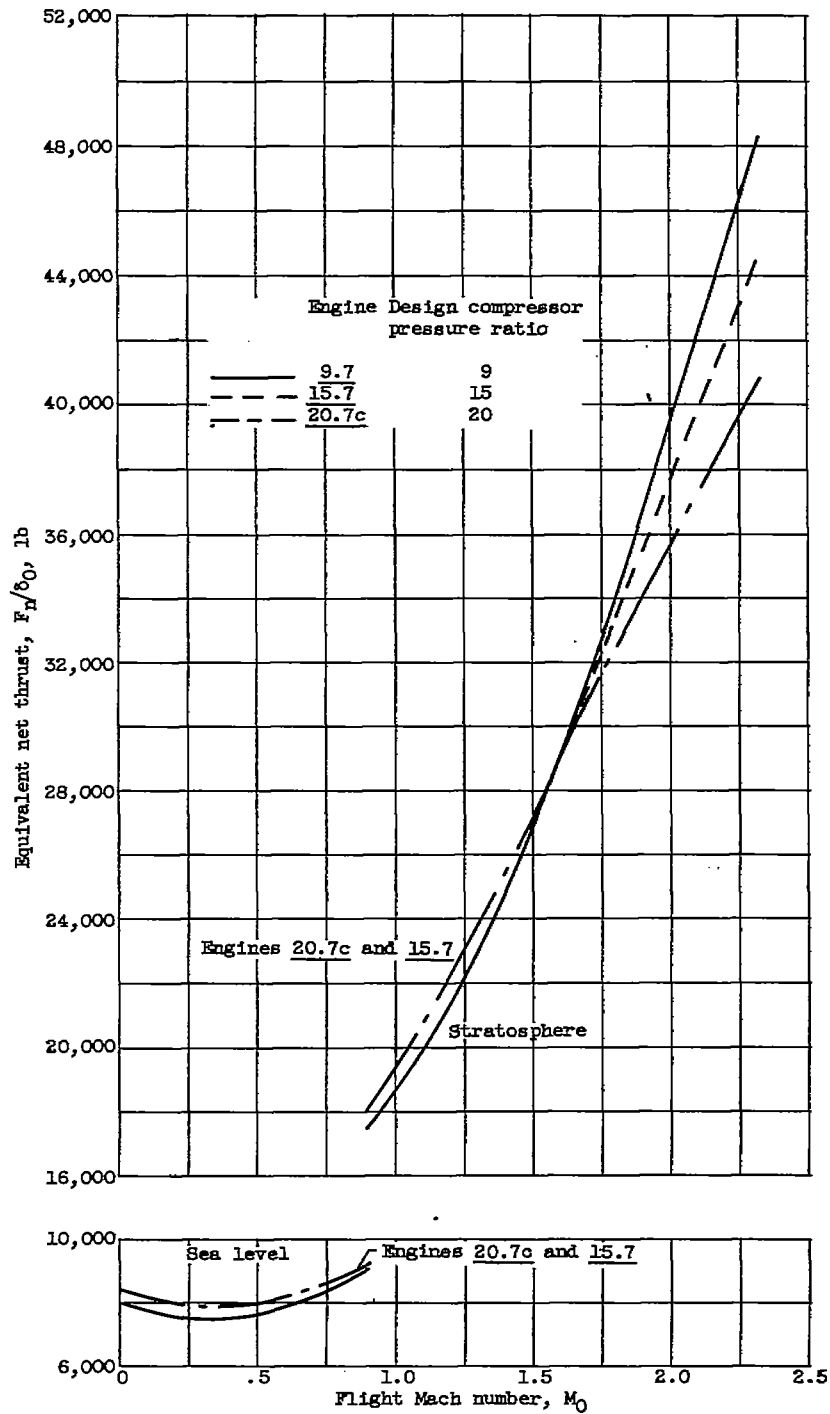
Figure 8. - Performance of engines 20.7c, 15.7, and 9.7 with afterburner inoperative.

3909



(b) Specific power.

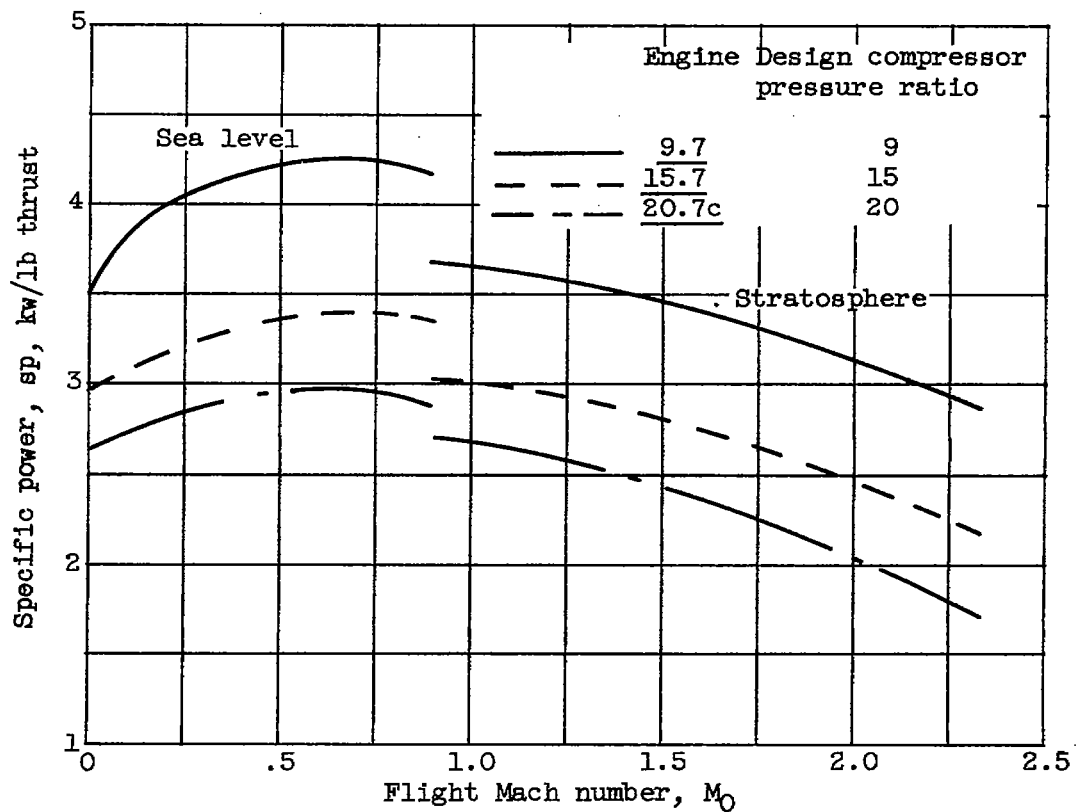
Figure 8. - Concluded. Performance of engines 20.7c, 15.7, and 9.7 with afterburner inoperative.



(a) Equivalent net thrust.

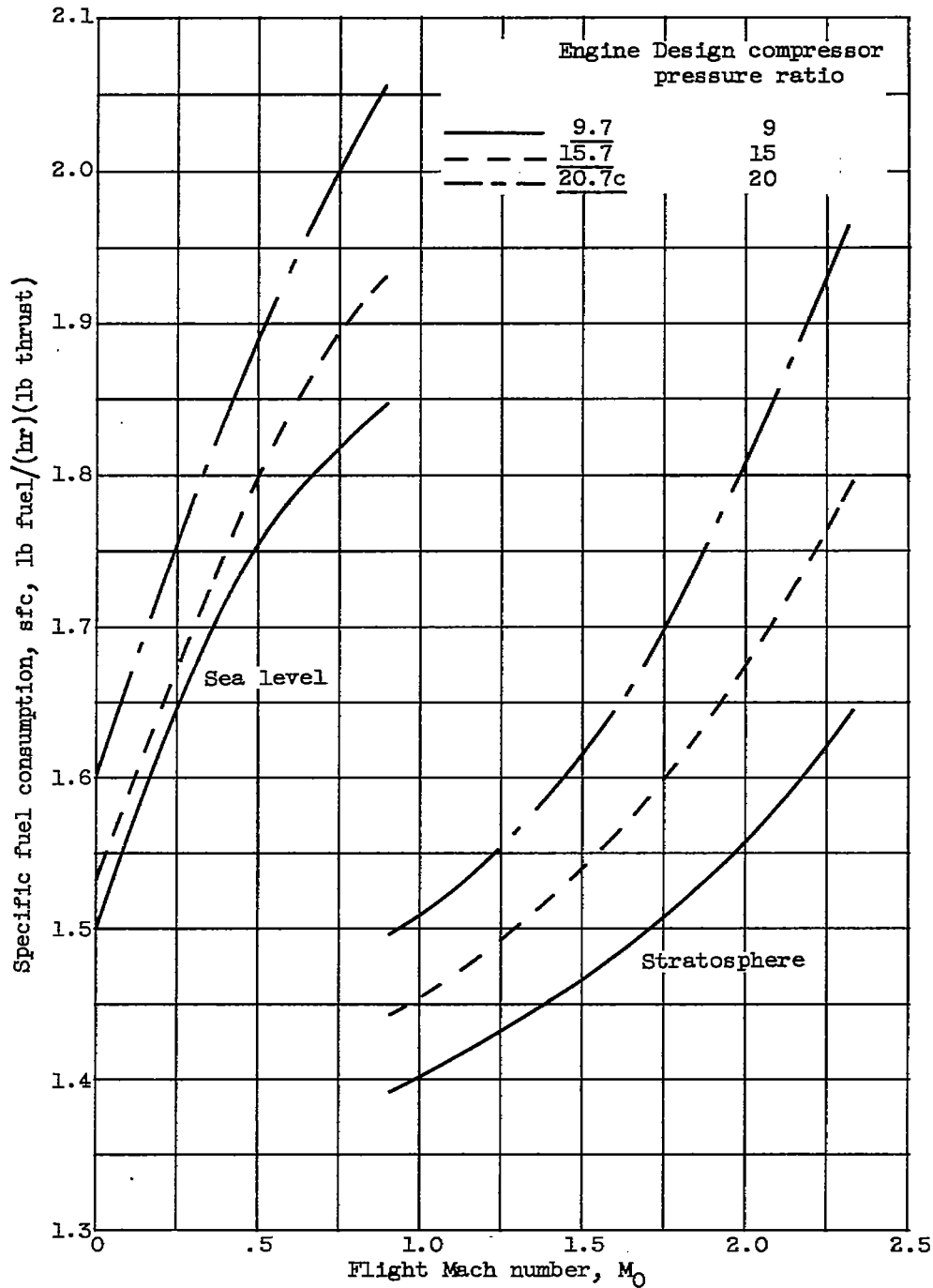
Figure 9. - Performance of engines 20.7c, 15.7, and 9.7 with afterburning at 3500° R.

5909



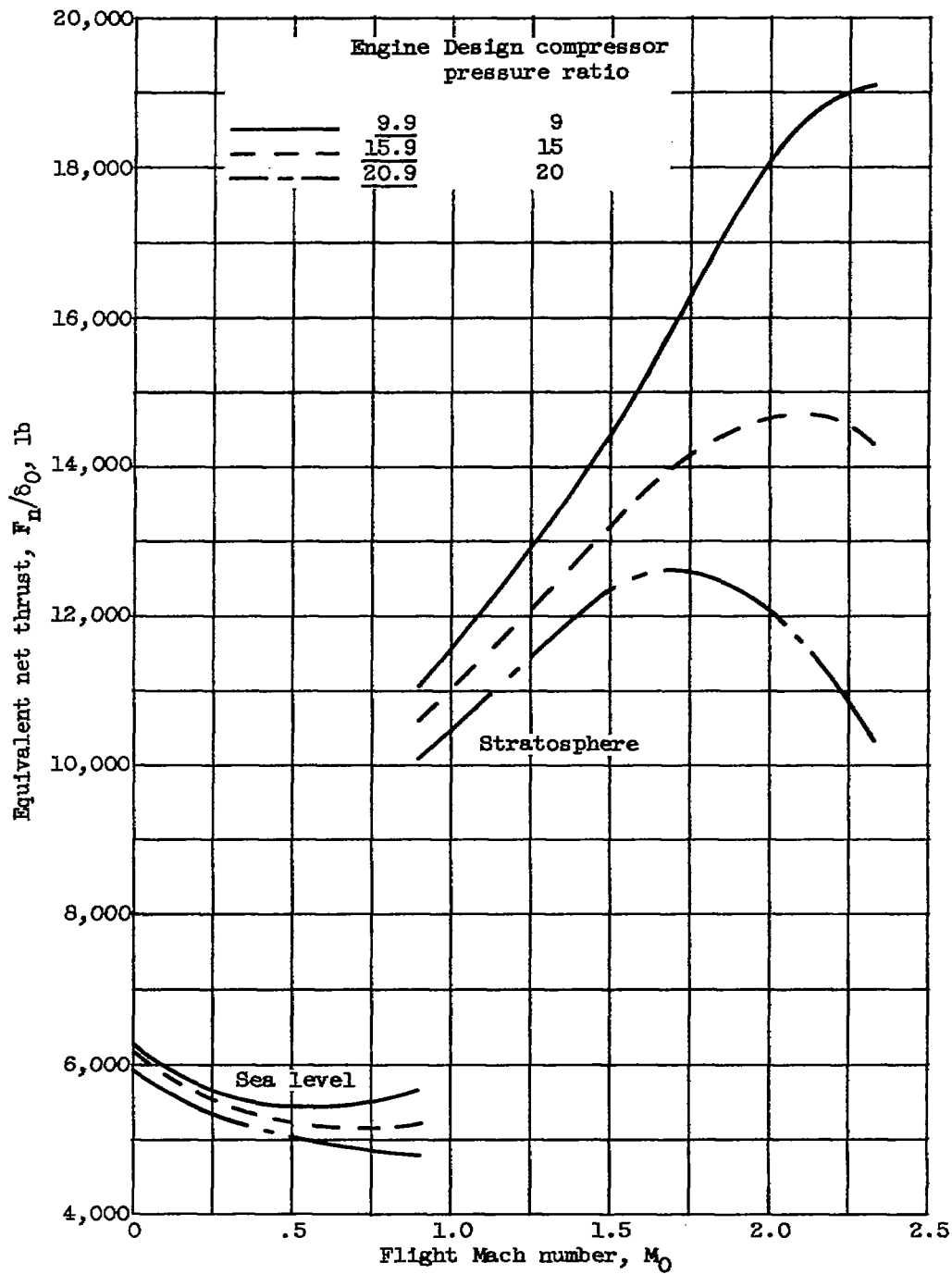
(b) Specific power.

Figure 9. - Continued. Performance of engines 20.7c, 15.7, and 9.7 with afterburning at 3500° R.



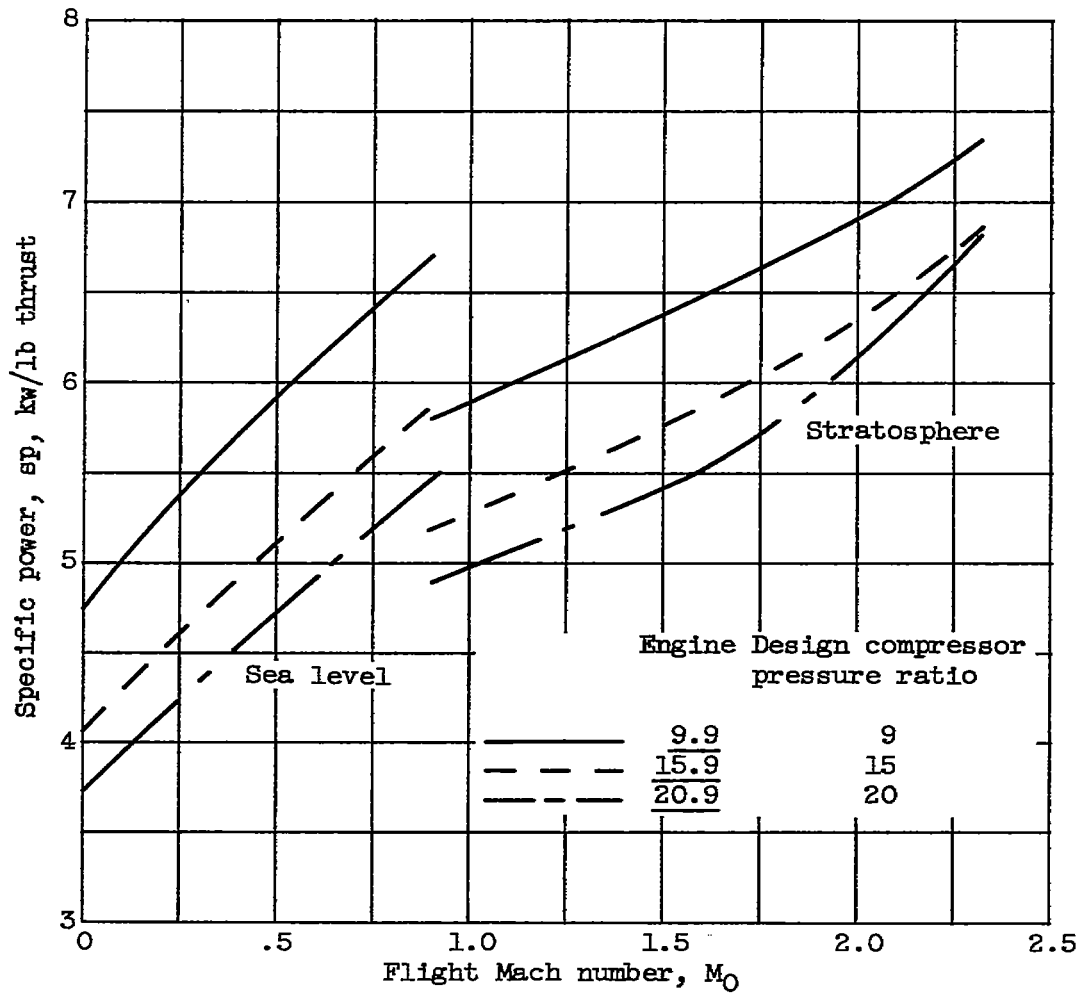
(c) Specific fuel consumption.

Figure 9. - Concluded. Performance of engines 20.7c, 15.7, and 9.7 with afterburning at 3500° R.



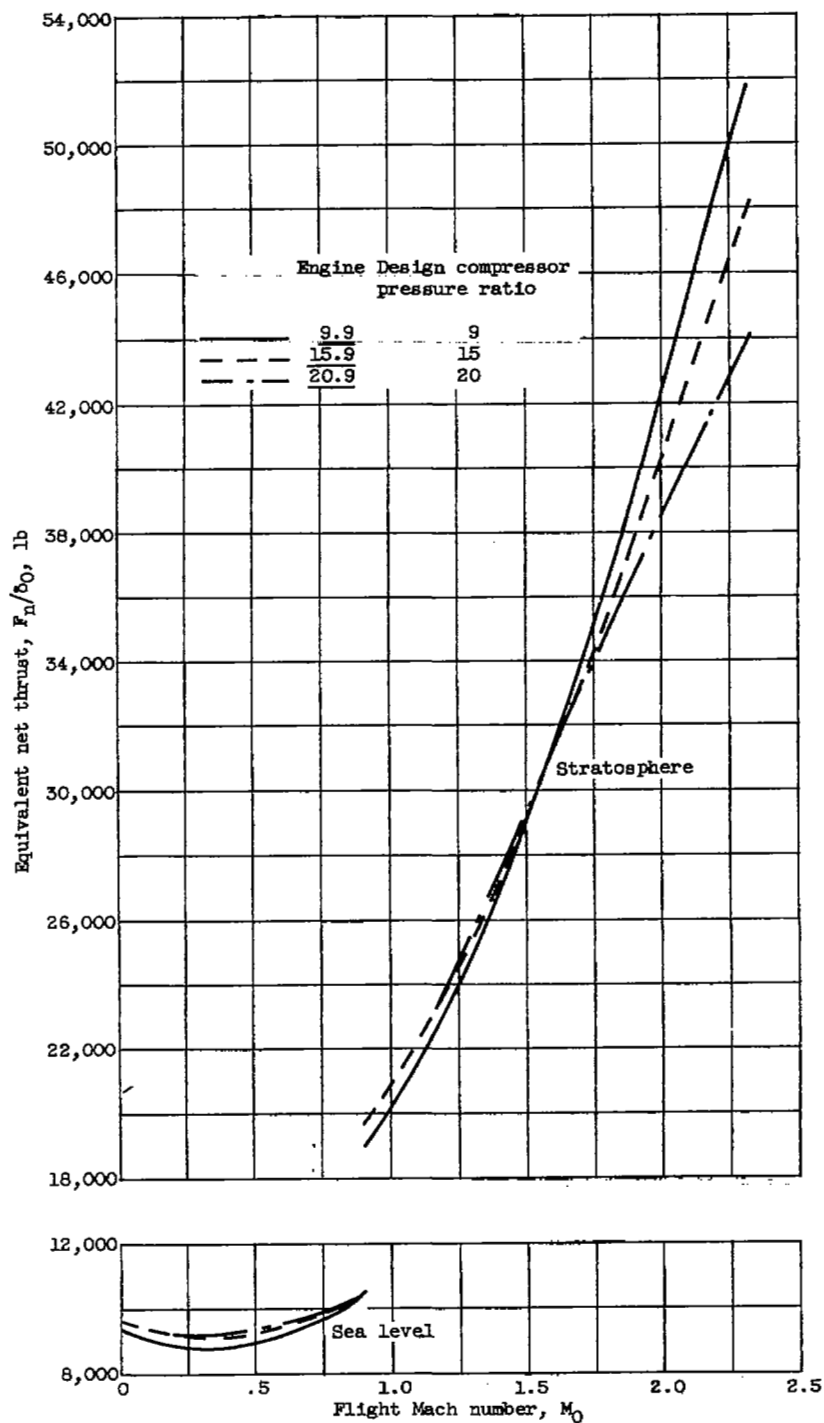
(a) Equivalent net thrust.

Figure 10. - Performance of engines 20.9, 15.9, and 9.9 with afterburner inoperative.



(b) Specific power.

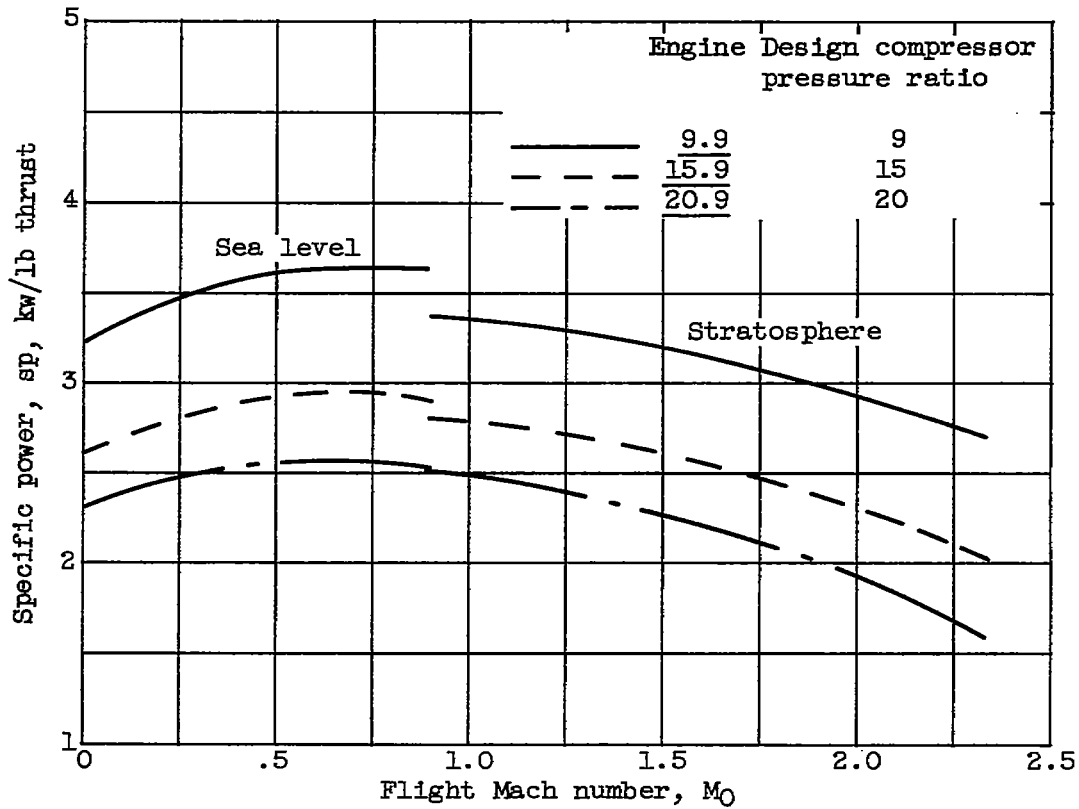
Figure 10. - Concluded. Performance of engines 20.9, 15.9, and 9.9 with afterburner inoperative.



(a) Equivalent net thrust.

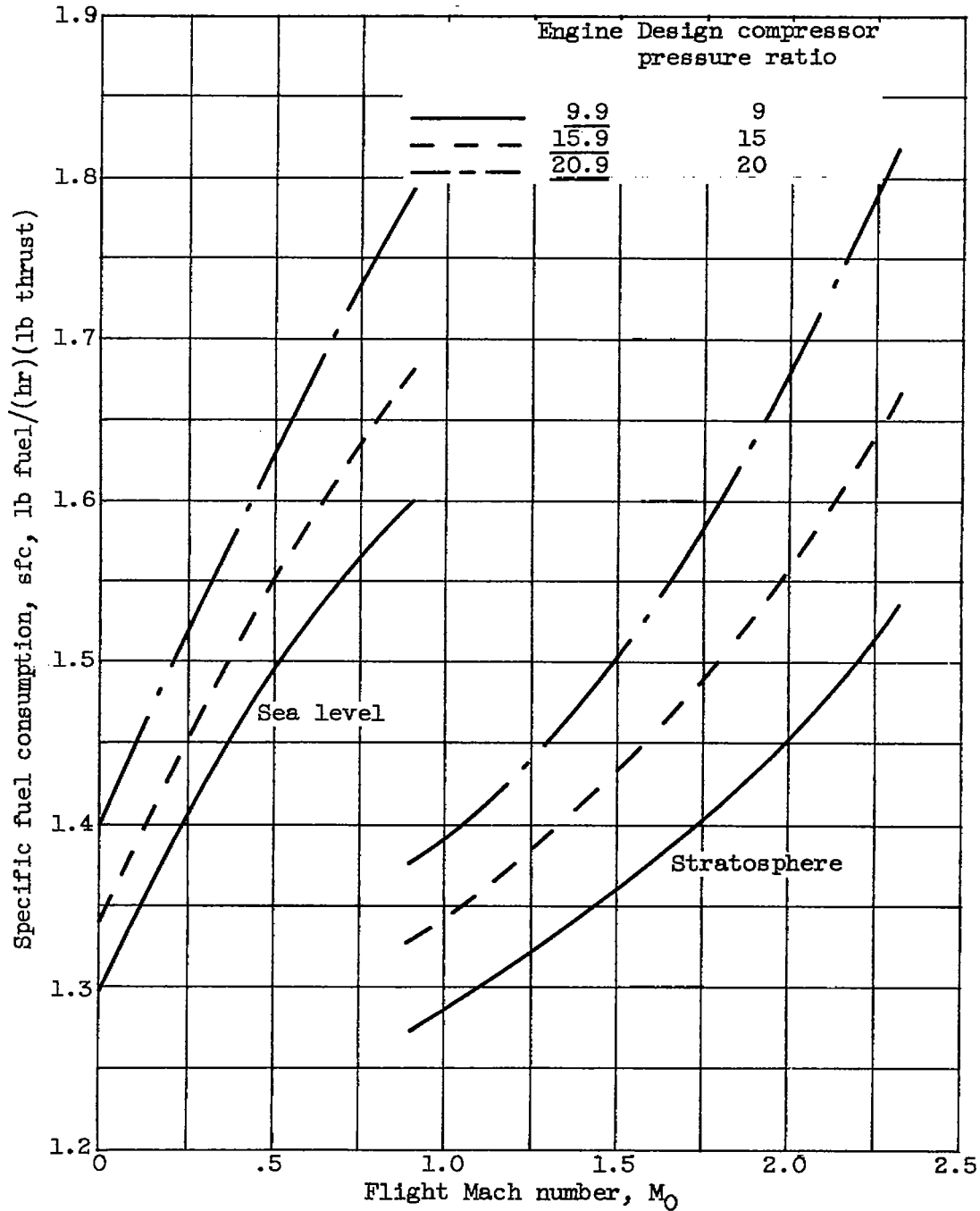
Figure 11. - Performance of engines 20.9, 15.9, and 9.9 with afterburning at 3500° R.

3909*



(b) Specific power.

Figure 11. - Continued. Performance of engines 20.9, 15.9, and 9.9 with afterburning at 3500° R.



(c) Specific fuel consumption.

Figure 11. - Concluded. Performance of engines 20.9, 15.9, and 9.9 with afterburning at 3500° R.

Engines, Turbojet	3.1.3
Compressors - Axial Flow	3.6.1.1
Compressors - Matching	3.6.3
Turbines - Axial Flow	3.7.1.1
Turbines - Matching	3.7.4
Dugan, James F., Jr.	

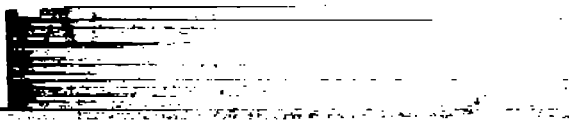
EFFECT OF DESIGN COMPRESSOR PRESSURE RATIO ON PERFORMANCE OF
HYPOTHETICAL TWO-SPOOL NUCLEAR-POWERED TURBOJET ENGINES

Abstract

For operation with the afterburner inoperative, the maximum equivalent net thrust for the 9:1 pressure-ratio engine is about 30 percent greater than that for the 15:1 pressure-ratio engine, and 51 percent greater than that for the 20:1 pressure-ratio engine. At each flight Mach number, however, the higher-pressure-ratio engines have the lower values of specific power (ratio of reactor power to engine net thrust) and require the smaller ducts downstream of the compressor exit.



3 1176 01436 5457

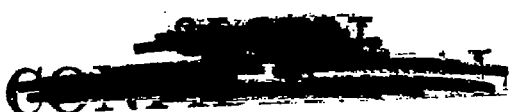


1

1

1

... ..



7